Sound & Vibration 2025, 59(4), 3381.
doi: https://doi.org/10.59400/sv3381

Article

Dynamic stability of a damped nonlinear axially moving beam resting on the nonlinear elastic foundation

Ghulam Yameen Mallah[1,*], Rajab Ali Malookani[2], Muhammad Memon[1], Muzaffar Bashir Arain[2], Izhar Ali Amur[3]

[1] Department of Basic Science and Related Studies , Quaid-e-Awam University of Engineering, Science & Technology, Nawabshah 67480, Pakistan
[2] Department of Mathematics and Statistics, Quaid-e-Awam University Engineering, Science & Technology, Nawabshah 67480, Pakistan
[3] Department of Basic Science and Related Studies, Shaheed Benazir Bhutto University, Shaheed Benazirabad 67480, Pakistan
*** Corresponding author:** Ghulam Yameen Mallah, gh.yameen@quest.edu.pk

CITATION

Mallah GY, Malookani RA, Memon M, et al. Dynamic stability of a damped nonlinear axially moving beam resting on the nonlinear elastic foundation. Sound & Vibration. 2025; 59(4): 3381. https://doi.org/10.59400/sv3381

ARTICLE INFO

Received: 12 June 2025
Revised: 7 August 2025
Accepted: 13 August 2025
Available online: 29 August 2025

Abstract: The stability of nonlinear transverse vibrations of an axially moving beam resting on a nonlinear elastic foundation is analysed, considering the effects of viscous damping and a harmonically varying time-dependent velocity around a low constant mean speed. The beam is assumed to have simply supported boundary conditions at both ends. The contribution of this paper is the combined study of damping, nonlinear foundation, and harmonic velocity variation on the stability of axially moving beams, which has not been studied before. The governing equation for the transverse dynamics is a nonlinear partial differential equation with variable coefficients, which is solved using the two-timescale perturbation method in combination with the Fourier series method. The stability of the system is investigated for both non-resonant and resonant cases by examining the influence of key parameters, including nonlinear bending stiffness, nonlinear elastic foundation and damping. The analysis reveals that an increase in nonlinear bending stiffness and nonlinear elastic foundation tends to destabilize the system, leading to growing oscillations and instability. In contrast, an increase in damping enhances stability, causing oscillations to decay over time and leading to an asymptotically stable response. Furthermore, validation was carried out through comparison with an existing model.

Keywords: axially moving beam; elastic foundation; viscous damping; two-time scales method; stability analysis

1. Introduction

Axially moving beam on elastic foundation represents a large class of mechanics in various disciplines of engineering such as aerospace [1] civil and mechanical engineering [2]. There are various mechanical and civil structures that represent engineering devices such as vibrating machines, pipelines, electric power lines, elevator cables, steel rod, saw-tooth blades, magnetic tapes, crane cables bridges and medical Nano robots [3]. Despite their numerous benefits and wide-ranging applications, the transverse vibrations have limited their efficiency and productivity. Various factors, such as wind forces, earthquakes and other external forces can induce vibrations which lead to potential damage or destroy the structures. For instance, vibrations in elevator cable [4], leakages in pipelines [5] and destruction of the Tacoma Narrows suspension bridge USA in 1940 completely [6] are few examples of damaged structures. To optimize the designs of such systems, numerous theoretical and experimental studies

have been conducted over the decades. Based on the system's flexibility and geometric characteristics, two models can be developed as string model [7] and beam model [8]. Extensive research has been conducted on the transverse dynamics of nonlinear vibration of beams on a nonlinear elastic foundation such as, the nonlinear vibrations of beam with cubic stiffness resting on a nonlinear spring foundation is examined [9], nonlinear dynamics of slightly curved beams are analyzed [10], the free and forced nonlinear dynamics of Kelvin-Voigt beam with nonlinear spring are discussed [11], vibration of axially moving beams with nonlinear viscoelastic foundations is analyzed [12], the nonlinear dynamic behavior of an axially moving beam with subjected to blast load in thermal environment is examined [13], positive position feedback is applied for vibration suppression in cantilever beams [14], a gyrostabilizer is used for modal control via dynamic inertia [15], thermal and follower force effects are analyzed on circular plates [16], energy transfer in axially loaded beams is studied on non-uniform foundations is studied in Xu et al. [17], piezoelectric layers were employed for active control of composite beams [18], a high-gain boundary feedback controller is developed for exponential stabilization [19], tuned mass dampers are implemented to attenuate nonlinear beam vibrations [20], nonlinear post-buckling dynamic of axially moving beam is explored under external loads [21], the complex periodic responses in beams are analyzed subjected to multi-frequency excitation [22], localized waves and moving-load effects are analyzed on damped Euler–Bernoulli beams [23], the stability of nonlinear forced vibration is investigated of an axially moving beam composed of two segments connected by a free internal hinge [24], the nonlinear transverse vibrations of a slightly curved hinged–hinged beam are analyzed under axial loading [25], the vibration suppression of a double-cable beam is investigated by nonlinear energy sinks [26], the large-amplitude vibration and buckling behavior of Euler–Bernoulli foam beams with viscoelasticity is examined resting on nonlinear elastic foundations [27], the nonlinear vibrations of deflection of beam with nonlinear elastic foundation are studied [28].

To analyze the dynamics of the system numerous numerical and analytical techniques are used, such as the perturbation methods [29], the lindstedt poincare method with frequency transformations [30], Galerkin's method [31], differential quadrature method [32], finite difference method [33] and averaging method [34]. The free vibrations of moving beams with elastic foundation are analyzed by Galerkin's method [35]. The chaotic behavior of beam-like models with foundation is obtained by the cosine-cosine function [36]. The homotopy perturbation method is used to analyze the behavior of axially loaded beam with variable elastic foundation [37] and for damped Mathieu equations under parametric excitation [38]. The classical multiple scales and multiple scales Lindstedt Poincare methods are employed to analyse the vibration [39] to find analytical solutions of nonlinear dynamic of beam with nonlinear elastic foundation. Approximate analytical solution is obtained of nonlinear vibration of beam with a nonlinear elastic foundation subject to moving load by the Galerkin's method and He's variational method [40]. The weakly nonlinear transverse vibrations of a convoy belt were analyzed by using a two-timescales method, revealing that nonlinearity stabilizes the system [41].

A thorough review of the literature shows that there are not many detailed studies on modes interaction for axially moving beams with nonlinear elastic foundations. Most research has focused on mode interactions in nonlinear beam vibrations but has not considered how a nonlinear elastic foundation affects these interactions. Studies have shown that different vibration modes interact within nonlinear systems but their behavior with a nonlinear foundation is not well understood. The novelty of this work lies in analyzing how nonlinear elastic foundations influence mode interactions in axially moving beams. This study incorporates damping and harmonic velocity variation simultaneously unlike prior studies [9, 12, 27], understanding these interactions is important for improving the stability and performance of axially moving beams in engineering. This contribution differs from earlier works [9, 12, 27] by jointly analyzing damping, nonlinear foundation, and harmonic velocity variation on modal interactions, which have not been considered together before. In this paper, the stability of nonlinear transverse vibrations of an axially moving beam with nonlinear elastic foundation under viscous damping is discussed with harmonically varying time dependent velocity and about low constant speed subject to the fixed boundary conditions under the effects nonlinear bending stiffness, nonlinear elastic foundation and internal damping. The governing equation of motion is discretized by the Fourier expansion method, then two-timescales perturbation method is used to the obtained infinite dimensional system of coupled ordinary differential equations.

The paper is structured as follows. In section 2, the mathematical formulation of the governing equations of nonlinear transverse vibrations of moving beam with elastic foundation and damping is presented. In section 3, construction of asymptotic approximations for examining the stability of the system with the method of two-timescales is given. In section 4, the stability of the system for interaction of different vibration modes in resonance regions is discussed. In section 5, the conclusions of the paper are presented.

2. Mathematical formulation

An axially transporting beam moving with the velocity $V(t)$ with the length L between two pulleys resting on non-linear elastic foundation is shown in **Figure 1**.

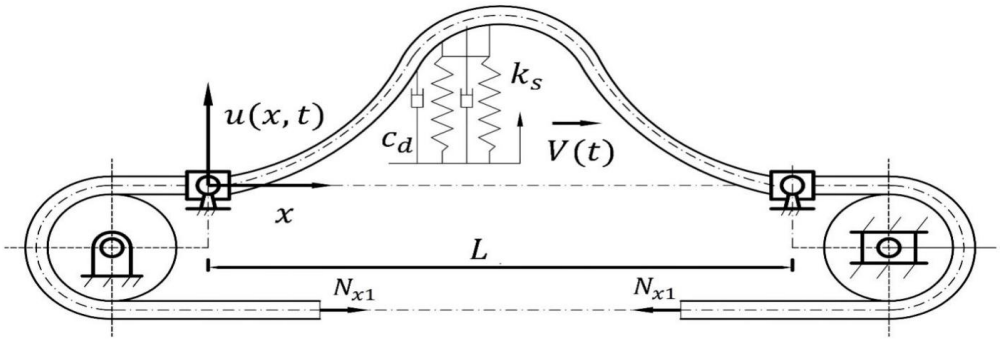

Figure 1. The schematic model of a moving beam [42].

The equations of motion that governs the nonlinear transversal vibrations of an axially transporting damped beam under elastic foundation is derived from Newton's

second law of motion [42] and can be represented as follows:

$$\begin{gathered}\rho A\left(\frac{\partial^2 u}{\partial t^2}+2V\frac{\partial^2 u}{\partial x\partial t}+V^2\frac{\partial^2 u}{\partial x^2}\right)+EI\frac{\partial^4 u}{\partial x^4}-N_{x1}\frac{\partial^2 u}{\partial x^2}-\\ \frac{EA}{2L}\frac{\partial^2 u}{\partial x^2}\int_0^L\left(\frac{\partial u}{\partial x}\right)^2 dx+k_{sl}u+k_{sn}u^3+c_d\left(\frac{\partial u}{\partial t}+V\frac{\partial u}{\partial x}\right)=0,\\ t\geq 0, 0<x<L,\end{gathered} \tag{1}$$

with simply supported boundary conditions:

$$u(0,t)=u(L,t)=0,\ u_{xx}(0,t)=u_{xx}(L,t)=0, t\geq 0 \tag{2}$$

and with initial conditions:

$$u(x,0)=f(x), u_t(x,0)=g(x).\ 0<x<L. \tag{3}$$

Where $u(x,t)$ is the transverse displacement with spatial axis x and time t, ρ is the density, A is cross-sectional area, I is moment of inertia, E is Young's modulus, k_{sl} is linear stiffness of foundation, k_{sn} is nonlinear stiffness of foundation, c_d is viscous damping, $N_{x1}=P_0+a\rho A\ V^2+(x-L)\rho A\dot{V}$ is the axial varying tension with P_0 is the initial axial varying tension and a is the axial support stiffness. The physical meaning of terms in Eq. (1), where $\frac{\partial^2 u}{\partial t^2}$ represents the local acceleration, $2V\frac{\partial^2 u}{\partial x\partial t}$ denotes the Coriolis acceleration due to the rotation, $V^2\frac{\partial^2 u}{\partial x^2}$ corresponds to centrifugal acceleration due to the beam curvature, $EI\frac{\partial^4 u}{\partial x^4}$ represent the bending stiffness to deformation, $N_{x1}\frac{\partial^2 u}{\partial x^2}$ indicates the influence of axial force on transverse displacement, $\frac{EA}{2L}\frac{\partial^2 u}{\partial x^2}\int_0^L\left(\frac{\partial u}{\partial x}\right)^2 dx$ express the Nonlinear bending effect due to stretching, $k_{sl}u$ represents the linear foundation stiffness due elastic restoring force, $k_{sn}u^3$ denotes the nonlinear foundation stiffness due to the cubic stiffness and $c_d\left(\frac{\partial u}{\partial t}+V\frac{\partial u}{\partial t}\right)$ describes the damping force.

The following dimensionless parameters are used to form the Eq. (1)–Eq. (3) dimensionless:

$$\begin{gathered}u^*=\frac{u}{\sqrt{\epsilon}L},\quad x^*=\frac{x}{L},\quad V^*=V\sqrt{\frac{\rho A}{P_0}},\ \ t^*=\frac{t}{L}\sqrt{\frac{P_0}{\rho A}},\quad k_{sl}^*=\frac{k_{sl}L^2}{\epsilon P_0},\\ k_{sn}^*=\frac{k_{sn}L^4}{\epsilon P_0}, c_d^*=\frac{c_d L}{\epsilon\sqrt{\rho A P_0}}, k_f=\sqrt{\frac{EI}{L^2P_0}},\quad P_1=\sqrt{\frac{EA}{\epsilon P_0}},\quad \kappa=1-a,\\ f(x)^*\ =\frac{f(x)}{\sqrt{\epsilon}L}, g(x)^*=g(x)\sqrt{\frac{\rho A}{\epsilon P_0}}.\end{gathered} \tag{4}$$

where ϵ with $0<\epsilon\ll 1$ is a bookkeeping parameter which indicates the smallness of transverse motion, elastic foundation and viscous damping. Substitution of Eq. (4) without asterisks into Eq. (1)–Eq. (3) yields the following non-dimensional form:

$$\begin{gathered}\frac{\partial^2 u}{\partial t^2}+2V\frac{\partial^2 u}{\partial x\partial t}+\left[\kappa V^2-(x-1)\dot{V}-1\right]\frac{\partial^2 u}{\partial x^2}+k_f^2\frac{\partial^4 u}{\partial x^4}=\\ \frac{1}{2}\epsilon P_1^2\frac{\partial^2 u}{\partial x^2}\int_0^1\left(\frac{\partial u}{\partial x}\right)^2 dx-\epsilon(k_{sl}u+k_{sn}u^3)-\epsilon c_d\left(\frac{\partial u}{\partial t}+V\frac{\partial u}{\partial x}\right),\\ t\geq 0, 0<x<1\end{gathered} \tag{5}$$

$$u(0,t)=u(1,t)=0, u_{xx}(0,t)=u_{xx}(1,t)=0, t\geq 0 \tag{6}$$

$$u(x,0)=f(x), u_t(x,0)=g(x), 0<x<1 \tag{7}$$

The axial speed is assumed about a low mean speed α_0 of order ϵ and harmonically

varying velocity $\epsilon\alpha$ with a frequency Ω as:

$$V(t) = \epsilon\alpha_0 + \epsilon\alpha \sin(\Omega t) \tag{8}$$

where α_0, α and Ω are constants with $\alpha_0 > 0$, $\Omega > 0$ and with a condition $\alpha_0 > |\alpha|$, that is the belt move forward axially.

3. Construction of the asymptotic approximations

In this section, a two-times perturbation combined with Fourier series approach is utilized to construct formal asymptotic approximations for the solution of initial-boundary value problem for Eq. (5)–Eq. (7). To satisfy the Dirichlet boundary conditions in Eq. (5), it is necessary to make all the terms odd [7]. So that even terms such as u_{xt} and xu_{xx} must be multiplied by the Fourier series of the functions $H(x)$ and $xH(x)$ respectively, and given as below:

$$H(x) = \begin{cases} -1 & -1 < x < 0 \\ 1 & 0 < x < 1 \end{cases} = \sum_{j=0}^{\infty} \frac{4}{(2j+1)\pi} \sin\left((2j+1)\pi x\right) \tag{9}$$

$$xH(x) = \frac{1}{2} - \sum_{j=0}^{\infty} \frac{4}{(2j+1)^2\pi^2} \cos\left((2j+1)\pi x\right) \tag{10}$$

By substituting Eq. (8)–Eq. (10) into Eq. (5), yields:

$$\begin{gathered} u_{tt} - u_{xx} + k_f^2 u_{xxxx} = \\ \epsilon[-2\left(\alpha_0 + \alpha\sin(\Omega t)\right) u_{xt} \textstyle\sum_{j=0}^{\infty} \frac{4}{(2j+1)\pi} \sin\left((2j+1)\pi x\right) + \\ \alpha\Omega\cos(\Omega t)\left(\frac{1}{2} - \textstyle\sum_{j=0}^{\infty} \frac{4}{(2j+1)^2\pi^2} \cos\left((2j+1)\pi x\right) - 1\right) u_{xx} + \\ \frac{1}{2}P_1^2 \frac{\partial^2 u}{\partial x^2} \int_0^1 \left(\frac{\partial u}{\partial x}\right)^2 dx - k_{sl}u - k_{sn}u^3 - c_d u_t] + O\left(\epsilon^2\right). \end{gathered} \tag{11}$$

To discretize the PDE in Eq. (11), the Fourier expansion method is used. The solution of Eq. (11) is assumed in the form as under:

$$u(x,t) = \sum_{n=1}^{\infty} u_n(t;\epsilon) \sin(n\pi x) \tag{12}$$

By putting Eq. (12) in Eq. (11), then multiplying the resulting equation with $\sin(k\pi x),\ k \in$ and then integrating w.r.t 'x' from 0 to 1 and observing the following orthogonality properties:

$$\int_0^1 \sin(n\pi x) \sin(k\pi x) dx = \begin{cases} 0, & \text{if } n \neq k \\ \frac{1}{2}, & \text{if } n = k \end{cases} \tag{13}$$

$$\int_0^1 \cos(n\pi x) \sin(j\pi x) \sin(k\pi x) dx = \begin{cases} 0, & \text{if } j \neq \pm n \pm k \\ \frac{1}{4}, & \text{if } j = k \pm n,\ \ j \geq 1 \\ -\frac{1}{4}, & \text{if } j = n - k,\ \ j = 1 \end{cases} \tag{14}$$

An infinite-dimensional system of coupled ordinary differential equations is

obtained,

$$\begin{gathered}\ddot{u}_k+((k\pi)^2+k_f^2(k\pi)^4)u_k=\epsilon[4\left(\alpha_0+\alpha\sin\left(\Omega t\right)\right)\{\textstyle\sum_{k=n-2j-1}-\\ \textstyle\sum_{k=2j+1+n}-\sum_{k=2j+1-n}\}\frac{n\dot{u}_n}{(2j+1)}+\\ 2\alpha\Omega\cos\left(\Omega t\right)\{\textstyle\sum_{k=n-2j-1}+\sum_{k=2j+1+n}-\sum_{k=2j+1-n}\}\frac{n^2u_n}{(2j+1)^2}-\\ \frac{k_{sn}}{4}\{3\textstyle\sum_{k=n+p-q}-3\sum_{k=-n-p+q}-\sum_{k=n+p+q}\}u_nu_pu_q-\\ \frac{k^2\pi^4P_1^2}{4}u_k\left(\textstyle\sum_{l=1}^{\infty}l^2u_l^2\right)+\frac{\alpha\Omega\cos\left(\Omega t\right)}{2}(k\pi)^2u_k-k_{sl}u_k-c_d\dot{u}_k]+O\left(\epsilon^2\right).\end{gathered}\tag{15}$$

In order to solve the Eq. (15), a two-timescales perturbation method will be used. Let's introduce the two-timescales, the fast timescales ($t_o=t$) and slow timescales ($t_1=\epsilon t$). With these timescales, the solution of Eq. (15) is assumed in the form:

$$u_k(t;\epsilon)=v_k\left(t_0,t_1;\epsilon\right)\tag{16}$$

The following time-derivatives are introduced:

$$\frac{du_k}{dt}=\frac{\partial v_k}{\partial t_0}+\epsilon\frac{\partial v_k}{\partial t_1}\tag{17}$$

$$\frac{d^2u_k}{dt^2}=\frac{\partial^2v_k}{\partial t_0^2}+2\epsilon\frac{\partial^2v_k}{\partial t_0\partial t_1}+\epsilon^2\frac{\partial^2v_k}{\partial t_1^2}\tag{18}$$

With Eq. (16)–Eq. (18), the Eq. (15) becomes:

$$\begin{gathered}\frac{\partial^2v_k}{\partial t_0^2}+2\epsilon\frac{\partial^2v_k}{\partial t_0\partial t_1}+\left((k\pi)^2+k_f^2(k\pi)^4\right)v_k=\\ \epsilon[4\left(\alpha_0+\alpha\sin\left(\Omega t\right)\right)\left\{\textstyle\sum_{k=n-2j-1}-\sum_{k=2j+1+n}-\sum_{k=2j+1-n}\right\}\frac{n}{(2j+1)}\frac{\partial v_n}{\partial t_0}\\ +2\alpha\Omega\cos\left(\Omega t\right)\left\{\textstyle\sum_{k=n-2j-1}+\sum_{k=2j+1+n}-\sum_{k=2j+1-n}\right\}\frac{n^2}{(2j+1)^2}v_n-\\ \frac{k_{sn}}{4}\left\{3\textstyle\sum_{k=n+p-q}-3\sum_{k=-n-p+q}-\sum_{k=n+p+q}\right\}v_nv_pv_q\\ -\frac{k^2\pi^4P_1^2}{4}v_k\left(\textstyle\sum_{l=1}^{\infty}l^2v_l^2\right)+\frac{\alpha\Omega\cos\left(\Omega t\right)}{2}(k\pi)^2v_k-k_{sl}v_k-c_d\frac{\partial v_k}{\partial t_0}]+O\left(\epsilon^2\right).\end{gathered}\tag{19}$$

Now assume:

$$v_k\left(t_0,t_1;\epsilon\right)=v_{k0}\left(t_0,t_1\right)+\epsilon v_{k1}\left(t_0,t_1\right)+O\left(\epsilon^2\right)\tag{20}$$

By putting Eq. (20) into Eq. (19) and making the coefficients of ϵ^0 and ϵ^1 equal to zero, it follows $O(1)$ problem and $O(\epsilon)$ problem respectively:

$$\frac{\partial^2v_{k0}}{\partial t_0^2}+\omega_k^2v_{k0}=0\tag{21}$$

$$\begin{gathered}\frac{\partial^2v_{k1}}{\partial t_0^2}+\omega_k^2v_{k1}=-2\frac{\partial^2v_{k0}}{\partial t_0\partial t_1}+\\ \left[\textstyle\sum_{k=n-2j-1}-\sum_{k=2j+1+n}-\sum_{k=2j+1-n}\right]\frac{4n(\alpha_0+\alpha\sin(\Omega t))}{(2j+1)}\frac{\partial v_{n0}}{\partial t_0}+\\ \left[\textstyle\sum_{k=n-2j-1}+\sum_{k=2j+1+n}-\sum_{k=2j+1-n}\right]\frac{2n^2\alpha\Omega\cos(\Omega t)}{(2j+1)^2}v_{n0}-\\ \frac{k_{sn}}{4}\left[3\textstyle\sum_{k=n+p-q}-3\sum_{k=-n-p+q}-\sum_{k=n+p+q}\right]v_{n0}v_{p0}v_{q0}-\\ \frac{k^2\pi^4P_1^2}{4}v_{k0}\left(\textstyle\sum_{l=1}^{\infty}l^2v_{l0}^2\right)+\left(\frac{\alpha\Omega\cos(\Omega t)}{2}(k\pi)^2-k_{sl}\right)v_{k0}-c_d\frac{\partial v_{k0}}{\partial t_0}.\end{gathered}\tag{22}$$

The solution of Eq. (21) is:

$$v_{k0}\left(t_0,t_1\right)=A_{k0}\left(t_1\right)\sin\left(\omega_k t_0\right)+B_{k0}\left(t_1\right)\cos\left(\omega_k t_0\right) \tag{23}$$

Where:

$$\omega_k=\sqrt{(k\pi)^2+k_f^2(k\pi)^4} \tag{24}$$

is the natural frequency of the beam system.

Substituting Eq. (23) on the right side of the Eq. (22), which results in:

$$\begin{gathered}
\frac{\partial^2 v_{k1}}{\partial t_0^2}+\omega_k^2 v_{k1}=-2\omega_k\left(\frac{dA_{k0}}{dt_1}\cos\left(\omega_k t_0\right)-\frac{dB_{k0}}{dt_1}\sin\left(\omega_k t_0\right)\right)+\\
\left[\sum_{k=n-2j-1}-\sum_{k=2j+1+n}-\sum_{k=2j+1-n}\right]\frac{2n\alpha\omega_n}{(2j+1)}[A_{n0}\{\sin\left(\Omega+\omega_n\right)t_0\\
+\sin\left(\Omega-\omega_n\right)t_0\}-B_{n0}\left\{\cos\left(\Omega-\omega_n\right)t_0-\cos\left(\Omega+\omega_n\right)t_0\right\}]+\\
\left[\sum_{k=n-2j-1}+\sum_{k=2j+1+n}-\sum_{k=2j+1-n}\right]\frac{n^2\alpha\Omega}{(2j+1)^2}[A_{n0}\{\sin\left(\Omega+\omega_n\right)t_0\\
-\sin\left(\Omega-\omega_n\right)t_0\}+B_{n0}\left\{\cos\left(\Omega-\omega_n\right)t_0+\cos\left(\Omega+\omega_n\right)t_0\right\}]-\\
\frac{k_{sn}}{16}\left[3\sum_{k=n+p-q}-3\sum_{k=-n-p+q}-\sum_{k=n+p+q}\right][A_{n0}A_{p0}B_{q0}\{\cos\left(\omega_n-\right.\\
\left.\omega_p+\omega_q\right)t_0+\cos\left(\omega_n-\omega_p-\omega_q\right)t_0-\cos\left(\omega_n+\omega_p+\omega_q\right)t_0-\\
\cos\left(\omega_n+\omega_p-\omega_q\right)t_0\}+A_{n0}B_{p0}A_{q0}\{\cos\left(\omega_n+\omega_p-\omega_q\right)t_0-\\
\cos\left(\omega_n+\omega_p+\omega_q\right)t_0+\cos\left(\omega_n-\omega_p-\omega_q\right)t_0-\cos\left(\omega_n-\omega_p+\omega_q\right)t_0\}+\\
B_{n0}A_{p0}A_{q0}\{\cos\left(\omega_n+\omega_p-\omega_q\right)t_0-\cos\left(\omega_n+\omega_p+\omega_q\right)t_0-\\
\cos\left(\omega_n-\omega_p-\omega_q\right)t_0+\cos\left(\omega_n-\omega_p+\omega_q\right)t_0\}+\\
B_{n0}B_{p0}B_{q0}\{\cos\left(\omega_n+\omega_p+\omega_q\right)t_0+\cos\left(\omega_n+\omega_p-\omega_q\right)t_0+\\
\cos\left(\omega_n-\omega_p+\omega_q\right)t_0+\cos\left(\omega_n-\omega_p-\omega_q\right)t_0\}+\\
A_{n0}A_{p0}A_{q0}\{\sin\left(\omega_n-\omega_p+\omega_q\right)t_0-\sin\left(\omega_n-\omega_p-\omega_q\right)t_0-\\
\sin\left(\omega_n+\omega_p+\omega_q\right)t_0+\sin\left(\omega_n+\omega_p-\omega_q\right)t_0\}+\\
A_{n0}B_{p0}B_{q0}\{\sin\left(\omega_n+\omega_p+\omega_q\right)t_0+\sin\left(\omega_n+\omega_p-\omega_q\right)t_0+\\
\sin\left(\omega_n-\omega_p+\omega_q\right)t_0+\sin\left(\omega_n-\omega_p-\omega_q\right)t_0\}+\\
B_{n0}A_{p0}B_{q0}\{\sin\left(\omega_n+\omega_p+\omega_q\right)t_0+\sin\left(\omega_n+\omega_p-\omega_q\right)t_0-\\
\sin\left(\omega_n-\omega_p+\omega_q\right)t_0-\sin\left(\omega_n-\omega_p-\omega_q\right)t_0\}+\\
B_{n0}B_{p0}A_{q0}\{\sin\left(\omega_n+\omega_p+\omega_q\right)t_0-\sin\left(\omega_n+\omega_p-\omega_q\right)t_0+\\
\sin\left(\omega_n-\omega_p+\omega_q\right)t_0-\sin\left(\omega_n-\omega_p-\omega_q\right)t_0\}]-\frac{k^2\pi^4P_1^2}{8}\{A_{k0}\sin\left(\omega_k\right)t_0+\\
B_{k0}\cos\left(\omega_k\right)t_0\}\sum_{l=1}^{\infty}l^2\left(A_{l0}^2+B_{l0}^2\right)-\frac{k^2\pi^4P_1^2}{16}\sum_{l=1}^{\infty}l^2\left(B_{l0}^2-A_{l0}^2\right)\\
[A_{k0}\left\{\sin\left(2\omega_l+\omega_k\right)t_0-\sin\left(2\omega_l-\omega_k\right)t_0\right\}+B_{k0}\{\cos\left(2\omega_l+\omega_k\right)t_0+\\
\cos\left(2\omega_l-\omega_k\right)t_0\}]-\frac{k^2\pi^4P_1^2}{8}\sum_{l=1}^{\infty}l^2A_{l0}B_{l0}[A_{k0}\{\cos\left(2\omega_l-\omega_k\right)t_0-\\
\cos\left(2\omega_l+\omega_k\right)t_0\}+B_{k0}\left\{\sin\left(2\omega_l+\omega_k\right)t_0+\sin\left(2\omega_l-\omega_k\right)t_0\right\}]-\\
k_{sl}\left\{A_{k0}\sin\left(\omega_k\right)t_0+B_{k0}\cos\left(\omega_k\right)t_0\right\}-c_d\omega_k\{A_{k0}\cos\left(\omega_{k0}\right)t_0-\\
B_{k0}\sin\left(\omega_k\right)t_0\}+\text{Non Secular Terms}.
\end{gathered} \tag{25}$$

4. Stability analysis

Since $\cos(\omega_k t_0)$ and $\sin(\omega_k t_0)$ are part of homogeneous solution of Eq. (25), so to eliminate secular terms, the coefficients of $\cos(\omega_k t_0)$ and $\sin(\omega_k t_0)$ on the right hand side in Eq. (25) must be equal to zero. That is if the velocity variation frequency Ω is within the neighborhood of sum and difference of two natural frequencies ω_k, the system's amplitude grows without bound. This phenomenon is known as resonance. From Eq. (25) it is observed that there are infinitely many resonances in the system if $\Omega = \pm\omega_n \pm \omega_k$. If the velocity variation frequency Ω is not within the neighborhood of the natural frequencies that cause the system's amplitude grow, so here only internal resonance occurs in equation (25) if $\Omega \neq \pm\omega_n \pm \omega_k$. This phenomenon is known as non-resonance.

4.1. When $\Omega \neq \pm\omega_n \pm \omega_k$ (Non-Resonant case)

In this case, the velocity variation frequency Ω is not within the neighborhood of any natural frequency of the system. By eliminating the secular terms in $O(1)-$ problem, that is, $v_{k1}(t_0, t_1)$, the following conditions are satisfied for the functions $A_{k0}(t_1)$ and $B_{k0}(t_1)$:

$$\begin{aligned}
\frac{dA_{k0}}{dt_1} &= -\frac{k_{sl}}{2\omega_k} B_{k0} - \frac{c_d}{2} A_{k0} - \frac{k^2\pi^4 P_1^2}{32\omega_k} B_{k0}\{k^2\left(A_{k0}^2 + B_{k0}^2\right) + \\
&\quad 2\sum_{l=1}^{\infty} l^2\left(A_{l0}^2 + B_{l0}^2\right)\} - \frac{3k_{sn}}{16\omega_k}\left(A_{p0}^2 + B_{p0}^2\right) B_{k0}, \\
\frac{dB_{k0}}{dt_1} &= \frac{k_{sl}}{2\omega_k} A_{k0} - \frac{c_d}{2} B_{k0} + \frac{k^2\pi^4 P_1^2}{32\omega_k} A_{k0}\{k^2\left(A_{k0}^2 + B_{k0}^2\right) + \\
&\quad 2\sum_{l=1}^{\infty} l^2\left(A_{l0}^2 + B_{l0}^2\right)\} + \frac{3k_{sn}}{16\omega_k}\left(A_{p0}^2 + B_{p0}^2\right) A_{k0}
\end{aligned} \tag{26}$$

To transform the system into the polar coordinates, let $A_{k0}(t_1) = r_k(t_1)\sin(\phi_k(t_1))$ and $B_{k0}(t_1) = r_k(t_1)\cos(\phi_k(t_1))$, so from Eq. (26) it follows that:

$$\begin{aligned}
\frac{dr_k}{dt_1} &= -\frac{c_d}{2} r_k, \\
\frac{d\phi_k}{dt_1} &= -\frac{k^2\pi^4 P_1^2}{32\omega_k}\left(k^2 r_k^2 + 2\sum_{l=1}^{\infty} l^2 r_l^2\right) - \frac{3k_{sn}}{16\omega_k} r_p^2 - \frac{k_{sl}}{2\omega_k}.
\end{aligned} \tag{27}$$

The solution of system in Eq. (27) is:

$$\begin{aligned}
r_k(t_1) &= Ce^{-\frac{1}{2}c_d t_1}, \\
\phi_k(t_1) &= \frac{k^2\pi^4 P_1^2}{32\omega_k c_d} C^2 e^{-c_d t_1}\left(k^2 + 2\sum_{l=1}^{\infty} l^2\right) + \frac{3k_{sn}}{16\omega_k c_d} C^2 e^{-c_d t_1} - \frac{k_{sl}}{2\omega_k} t_1 + \widetilde{C},
\end{aligned} \tag{28}$$

Where C and $\widetilde{C}$ are arbitrary constants.

It can be observed from Eq. (28), that system will exponentially decrease with increase of c_d, while P_1, k_{sn} and k_{sl} effect the frequency of the system, furthermore, to see the behavior of the system the graphs are made in phase portraits. The phase portraits of the system in Eq. (26) are shown under the effect of bending stiffness P_1, nonlinear elastic foundation k_{sn} and damping c_d, while keeping other parameters fixed to 0.003. **Figure 2** shows the effect of bending stiffness. In **Figure 2a**, for smaller values of P_1, all trajectories move toward the origin, indicating that the system loses energy over time and stabilizes at equilibrium. In **Figure 2b**, for larger values of P_1,

the system becomes oscillatory, meaning that the increased stiffness sustains periodic motion instead of allowing the system to settle at the origin. **Figure 3** illustrates the impact of the nonlinear elastic foundation. In **Figure 3a**, for smaller values of k_{sn}, all trajectories spiral inward to the origin, implying that the system undergoes damping and eventually reaches equilibrium. In **Figure 3b**, for larger values of k_{sn}, the system exhibits periodic motion near the origin, indicating that a stronger nonlinear foundation provides sufficient elastic resistance to sustain oscillations. **Figure 4** illustrates the impact of the damping parameter c_d. In **Figure 4a**, for smaller values of c_d, the system remains oscillatory, suggesting that the damping effect is weak and unable to suppress vibrations. In **Figure 4b**, for relatively larger values of c_d, all trajectories converge asymptotically to the origin, demonstrating that increased damping enhances energy dissipation, leading to the decay of oscillations and eventual stabilization at equilibrium. Physically, higher nonlinear foundation stiffness amplifies restoring forces that sustain oscillations, while damping dissipates energy, suppressing resonance amplification and stabilizing the beam.

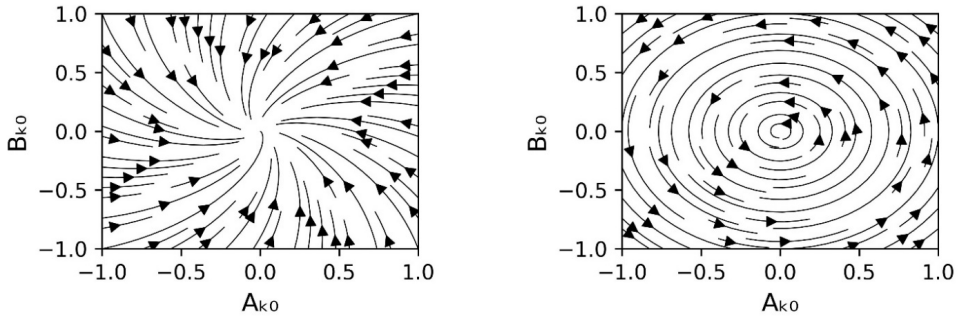

(a) **(b)**

Figure 2. Phase portraits when: **(a)** $P_1 = 0.0001$; **(b)** $P_1 = 0.1$.

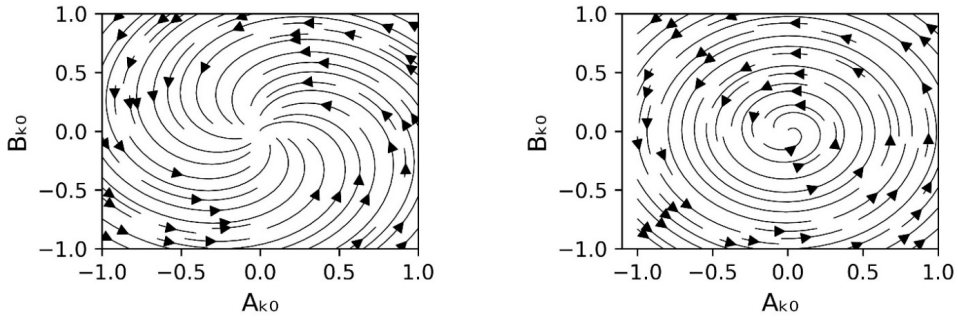

(a) **(b)**

Figure 3. Phase portraits when: **(a)** $k_{sn} = 0.0001$; **(b)** $k_{sn} = 3$.

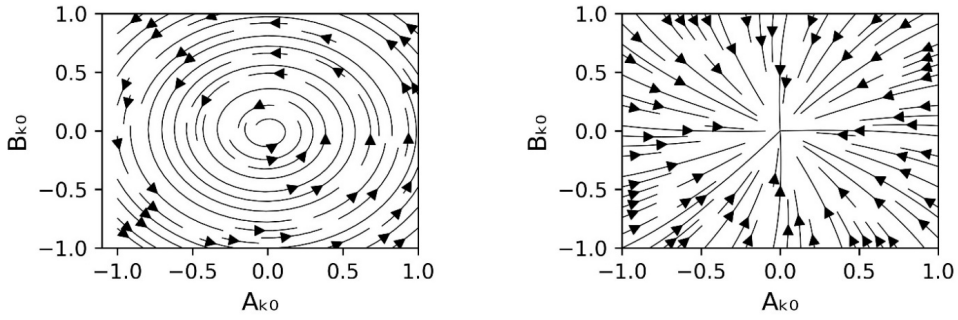

(a) **(b)**

Figure 4. Phase portraits when: **(a)** $c_d = 0.0001$; **(b)** $c_d = 0.1$.

4.2. When $\Omega = \pm\omega_n \pm \omega_k$ (Resonant case)

In this paper, the following resonant cases are considered [41]. 1. $\Omega = \omega_2 - \omega_1$, 2. $\Omega = \omega_3 - \omega_2$, 3. $\Omega = \omega_2 + \omega_1$ *and* 4. $\Omega = \omega_3 + \omega_2$ with detuning parameter ϕ and is of $O(1)$, where Ω denote the excitation frequency of axial velocity variation, and ω_1, ω_2, ω_3 the natural frequencies. The detuning parameter ϕ is defined as the deviation from the resonance region. For non-linear elastic foundation, it is shown in **Appendix A** that when $\Omega = \omega_2 \pm \omega_1$, if $k = 1$, $n = 2$ then $p = 1$, $q = 2$ and if $k = 2$, $n = 1$ then $p = 2$, $q = 1$. Similarly, when $\Omega = \omega_3 \pm \omega_2$, if $k = 2$, $n = 3$ then $p = 2$, $q = 3$ and if $k = 3$, $n = 2$ then $p = 3$, $q = 2$.

Case 1. When $\Omega = \omega_2 - \omega_1 + \epsilon\phi$

It is shown in **Appendix B** that by substituting $\Omega = \omega_2 - \omega_1 + \epsilon\phi$ in Eq. (25) and making the terms equal to zero that cause resonances, the following coupled ordinary equations are obtained:

$$
\begin{aligned}
\frac{dA_{10}}{dt_1} &= -\frac{4\alpha}{9\omega_1}\left(\omega_2 - 4\omega_1\right)A_{20}\sin\left(\phi t_1\right) + \frac{4\alpha}{9\omega_1}\left(\omega_2 - 4\omega_1\right)B_{20}\cos\left(\phi t_1\right) - \\
&\frac{\pi^4 P_1^2}{32\omega_1}B_{10}\left\{\left(A_{10}^2 + B_{10}^2\right) + 2\sum_{l=1}^{\infty} l^2\left(A_{l0}^2 + B_{l0}^2\right)\right\} - \frac{3k_{sn}}{16\omega_1}\left(A_{20}^2 + B_{20}^2\right)B_{10} \\
&- \frac{k_{sl}}{2\omega_1}B_{10} - \frac{c_d}{2}A_{10}, \\
\frac{dB_{10}}{dt_1} &= -\frac{4\alpha}{9\omega_1}\left(\omega_2 - 4\omega_1\right)A_{20}\cos\left(\phi t_1\right) - \frac{4\alpha}{9\omega_1}\left(\omega_2 - 4\omega_1\right)B_{20}\sin\left(\phi t_1\right) + \\
&\frac{\pi^4 P_1^2}{32\omega_1}A_{10}\left\{\left(A_{10}^2 + B_{10}^2\right) + 2\sum_{l=1}^{\infty} l^2\left(A_{l0}^2 + B_{l0}^2\right)\right\} + \frac{3k_{sn}}{16\omega_1}\left(A_{20}^2 + B_{20}^2\right)A_{10} \\
&+ \frac{k_{sl}}{2\omega_1}A_{10} - \frac{c_d}{2}B_{10}, \\
\frac{dA_{20}}{dt_1} &= \frac{4\alpha}{9\omega_2}\left(\omega_2 - 4\omega_1\right)A_{10}\sin\left(\phi t_1\right) + \frac{4\alpha}{9\omega_2}\left(\omega_2 - 4\omega_1\right)B_{10}\cos\left(\phi t_1\right) - \\
&\frac{\pi^4 P_1^2}{4\omega_2}B_{20}\left\{2\left(A_{20}^2 + B_{20}^2\right) + \sum_{l=1}^{\infty} l^2\left(A_{l0}^2 + B_{l0}^2\right)\right\} - \frac{3k_{sn}}{16\omega_2}\left(A_{10}^2 + B_{10}^2\right)B_{20} \\
&- \frac{k_{sl}}{2\omega_2}B_{20} - \frac{c_d}{2}A_{20}, \\
\frac{dB_{20}}{dt_1} &= -\frac{4\alpha}{9\omega_2}\left(\omega_2 - 4\omega_1\right)A_{10}\cos\left(\phi t_1\right) + \frac{4\alpha}{9\omega_2}\left(\omega_2 - 4\omega_1\right)B_{10}\sin\left(\phi t_1\right) + \\
&\frac{\pi^4 P_1^2}{4\omega_2}A_{20}\left\{2\left(A_{20}^2 + B_{20}^2\right) + \sum_{l=1}^{\infty} l^2\left(A_{l0}^2 + B_{l0}^2\right)\right\} + \frac{3k_{sn}}{16\omega_2}\left(A_{10}^2 + B_{10}^2\right)A_{20} \\
&+ \frac{k_{sl}}{2\omega_2}A_{20} - \frac{c_d}{2}B_{20}.
\end{aligned}
\tag{29}
$$

To transform the system into the polar coordinates, let $A_{k0}(t_1) = r_k(t_1)$

$\sin(\phi_k(t_1))$ and $B_{k0}(t_1) = r_k(t_1)\cos(\phi_k(t_1))$, so from Eq. (29) yields:

$$\begin{aligned}
\frac{dr_1}{dt_1} &= -\frac{c_d}{2}r_1 - \frac{4\alpha(\omega_2-4\omega_1)}{9\omega_1}r_2\sin(\phi_2-\phi_1+\phi t_1),\\
\frac{dr_2}{dt_1} &= -\frac{c_d}{2}r_2 + \frac{4\alpha(\omega_2-4\omega_1)}{9\omega_2}r_1\sin(\phi_2-\phi_1+\phi t_1),\\
\frac{d\phi_1}{dt_1} &= \frac{4\alpha(\omega_2-4\omega_1)r_2}{9\omega_1 r_1}\cos(\phi_2-\phi_1+\phi t_1) - \frac{\pi^4 P_1^2}{32\omega_1}\left(r_1^2+2\sum_{l=1}^{\infty}l^2 r_l^2\right)\\
&\quad -\frac{3k_{sn}}{16\omega_1}r_2^2 - \frac{k_{sl}}{2\omega_1},\\
\frac{d\phi_2}{dt_1} &= \frac{4\alpha(\omega_2-4\omega_1)r_1}{9\omega_2 r_2}\cos(\phi_2-\phi_1+\phi t_1) - \frac{\pi^4 P_1^2}{4\omega_2}\left(2r_2^2+\sum_{l=1}^{\infty}l^2 r_l^2\right)\\
&\quad -\frac{3k_{sn}}{16\omega_2}r_1^2 - \frac{k_{sl}}{2\omega_2}.
\end{aligned} \tag{30}$$

From first two equations in Eq. (30); which results in that $\omega_1 r_1^2+\omega_2 r_2^2 = c_1 e^{-c_d t_1}$, where c_1 is constant of integration. Now let $\Phi(t_1) = \phi_2(t_1) - \phi_1(t_1) + \phi t_1$, so from the last Eq. (30) it follows that:

$$\begin{aligned}
\frac{dr_1}{dt_1} &= -\frac{c_d}{2}r_1 + \frac{4\alpha(4\omega_1-\omega_2)}{9\omega_1}\sqrt{\frac{c_1 e^{-c_d t_1}-\omega_1 r_1^2}{\omega_2}}\sin(\Phi),\\
\frac{d\Phi}{dt_1} &= \phi + \frac{4\alpha(4\omega_1-\omega_2)}{9}\left(\frac{\sqrt{c_1 e^{-c_d t_1}-\omega_1 r_1^2}}{\omega_1\sqrt{\omega_2}r_1} - \frac{r_1}{\sqrt{\omega_2}\sqrt{c_1 e^{-c_d t_1}-\omega_1 r_1^2}}\right)\cos(\Phi)+\\
&\quad \pi^4 P_1^2\{\left(\frac{3}{32\omega_1}-\frac{1}{4\omega_2}\right)r_1^2 + \left(\frac{1}{4\omega_1}-\frac{3}{2\omega_2}\right)\frac{c_1 e^{-c_d t_1}-\omega_1 r_1^2}{\omega_2}+\\
&\quad \left(\frac{1}{16\omega_1}-\frac{1}{4\omega_2}\right)C^2 e^{-c_d t_1}\sum_{l=3}^{\infty}l^2\} + \frac{3k_{sn}}{16}\left(\frac{c_1 e^{-c_d t_1}-\omega_1 r_1^2}{\omega_1\omega_2} - \frac{r_1^2}{\omega_2}\right)+\\
&\quad \frac{k_{sl}}{2}\left(\frac{1}{\omega_1}-\frac{1}{\omega_2}\right).
\end{aligned} \tag{31}$$

and $\dot{r}_k = -\frac{c_d}{2}r_k$ for $k = 3,4,5,\ldots. \Rightarrow r_k(t_1) = Ce^{-c_d t_1}$.

Stability of beam in difference-type resonance of interaction 1st and 2nd modes is shown by phase portraits of the system in Eq. (31) under the effect of bending stiffness P_1, nonlinear elastic foundation k_{sn} and damping c_d, while keeping other parameters fixed to 0.003.

Figure 5 depicts the behaviour of the beam under the effect of bending stiffness P_1. When P_1 is relatively small, all trajectories indicate that the system tends to rotate around certain fixed points, as observed in **Figure 5a**. In **Figure 5b**, for larger values of P_1, all trajectories move away from the fixed points, causing the system to become unstable. **Figure 6** illustrates the effects of the nonlinear elastic foundation k_{sn}. In **Figure 6a**, the trajectories around the fixed points show that the system undergoes periodic oscillations for smaller values of k_{sn}. However, for larger values of k_{sn}, the instability region expands, as depicted in **Figure 6b**. **Figure 7** presents the effects of the damping parameter c_d. In **Figure 7a**, all trajectories move around the fixed points, indicating sustained motion. In **Figure 7b**, for larger values of c_d, all trajectories spiral inward toward the fixed points, demonstrating that the system becomes asymptotically stable due to enhanced damping. So, the instability increases with greater bending stiffness P_1 and nonlinear foundation stiffness k_{sn}, while stability increases with higher damping c_d.

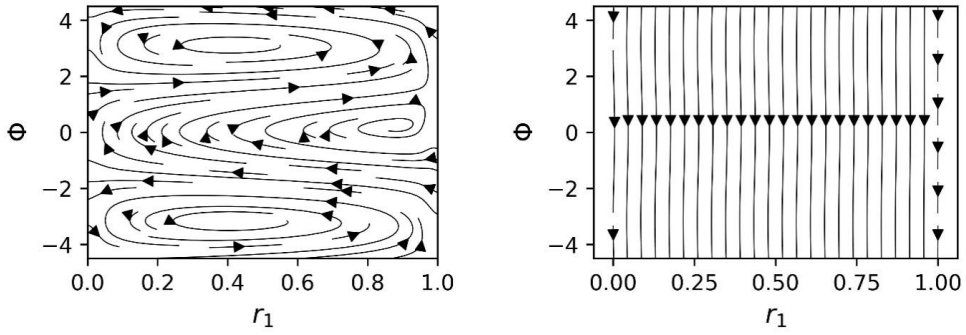

(a) **(b)**

Figure 5. Phase portraits when: **(a)** $P_1 = 0.0001$; **(b)** $P_1 = 0.1$.

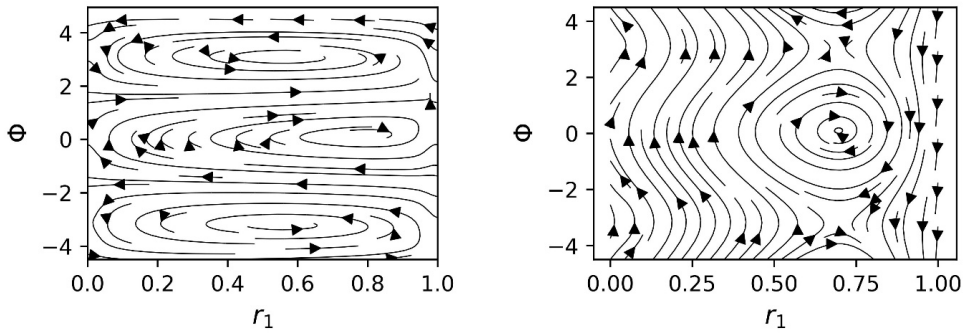

(a) **(b)**

Figure 6. Phase portraits when: **(a)** $k_{sn} = 0.0001$; **(b)** $k_{sn} = 8$.

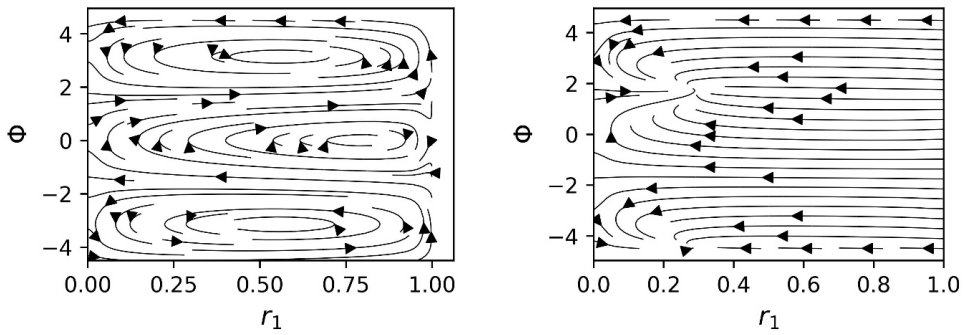

(a) **(b)**

Figure 7. Phase portraits when: **(a)** $c_d = 0.0001$; **(b)** $c_d = 0.1$.

Case 2. When $\Omega = \omega_2 + \omega_1 + \epsilon\phi$

Substituting $\Omega = \omega_2 + \omega_1 + \epsilon\phi$ in Eq. (25) and making the terms equal to zero that cause resonances, the following coupled ordinary equations are obtained:

$$\begin{gathered}
\frac{dA_{10}}{dt_1} = -\frac{4\alpha}{9\omega_1}\left(\omega_2+4\omega_1\right)A_{20}\sin\left(\phi t_1\right)+\frac{4\alpha}{9\omega_1}\left(\omega_2+4\omega_1\right)B_{20}\cos\left(\phi t_1\right)- \\
\frac{\pi^4P_1^2}{32\omega_1}B_{10}\left\{\left(A_{10}^2+B_{10}^2\right)+2\sum_{l=1}^{\infty}l^2\left(A_{l0}^2+B_{l0}^2\right)\right\}-\frac{3k_{sn}}{16\omega_1}\left(A_{20}^2+B_{20}^2\right)B_{10} \\
-\frac{k_{sl}}{2\omega_1}B_{10}-\frac{c_d}{2}A_{10}, \\
\frac{dB_{10}}{dt_1} = \frac{4\alpha}{9\omega_1}\left(\omega_2+4\omega_1\right)A_{20}\cos\left(\phi t_1\right)+\frac{4\alpha}{9\omega_1}\left(\omega_2+4\omega_1\right)B_{20}\sin\left(\phi t_1\right)+ \\
\frac{\pi^4P_1^2}{32\omega_1}A_{10}\left\{\left(A_{10}^2+B_{10}^2\right)+2\sum_{l=1}^{\infty}l^2\left(A_{l0}^2+B_{l0}^2\right)\right\}+\frac{3k_{sn}}{16\omega_1}\left(A_{20}^2+B_{20}^2\right)A_{10} \\
+\frac{k_{sl}}{2\omega_1}A_{10}-\frac{c_d}{2}B_{10}, \\
\frac{dA_{20}}{dt_1} = -\frac{4\alpha}{9\omega_2}\left(\omega_2+4\omega_1\right)A_{10}\sin\left(\phi t_1\right)+\frac{4\alpha}{9\omega_2}\left(\omega_2+4\omega_1\right)B_{10}\cos\left(\phi t_1\right)- \\
\frac{\pi^4P_1^2}{4\omega_2}B_{20}\left\{2\left(A_{20}^2+B_{20}^2\right)+\sum_{l=1}^{\infty}l^2\left(A_{l0}^2+B_{l0}^2\right)\right\}-\frac{3k_{sn}}{16\omega_2}\left(A_{10}^2+B_{10}^2\right)B_{20} \\
-\frac{k_{sl}}{2\omega_2}B_{20}-\frac{c_d}{2}A_{20}, \\
\frac{dB_{20}}{dt_1} = \frac{4\alpha}{9\omega_2}\left(\omega_2+4\omega_1\right)A_{10}\cos\left(\phi t_1\right)+\frac{4\alpha}{9\omega_2}\left(\omega_2+4\omega_1\right)B_{10}\sin\left(\phi t_1\right)+ \\
\frac{\pi^4P_1^2}{4\omega_2}A_{20}\left\{2\left(A_{20}^2+B_{20}^2\right)+\sum_{l=1}^{\infty}l^2\left(A_{l0}^2+B_{l0}^2\right)\right\}+\frac{3k_{sn}}{16\omega_2}\left(A_{10}^2+B_{10}^2\right)A_{20} \\
+\frac{k_{sl}}{2\omega_2}A_{20}-\frac{c_d}{2}B_{20}.
\end{gathered} \tag{32}$$

To transform the system into the polar coordinates, let $A_{k0}(t_1) = r_k\left(t_1\right)\sin\left(\phi_k\left(t_1\right)\right)$ and $B_{k0}(t_1) = r_k\left(t_1\right)\cos\left(\phi_k\left(t_1\right)\right)$, so from Eq. (32) it follows that:

$$\begin{gathered}
\frac{dr_1}{dt_1} = -\frac{c_d}{2}r_1+\frac{4\alpha(\omega_2+4\omega_1)}{9\omega_1}r_2\sin\left(\phi_2+\phi_1+\phi t_1\right), \\
\frac{dr_2}{dt_1} = -\frac{c_d}{2}r_2+\frac{4\alpha(\omega_2+4\omega_1)}{9\omega_2}r_1\sin\left(\phi_2+\phi_1+\phi t_1\right), \\
\frac{d\phi_1}{dt_1} = \frac{4\alpha(\omega_2+4\omega_1)r_2}{9\omega_1 r_1}\cos\left(\phi_2+\phi_1+\phi t_1\right)-\frac{\pi^4P_1^2}{32\omega_1}\left(r_1^2+2\sum_{l=1}^{\infty}l^2r_l^2\right)-\frac{3k_{sn}}{16\omega_1}r_2^2-\frac{k_{sl}}{2\omega_1}, \\
\frac{d\phi_2}{dt_1} = \frac{4\alpha(\omega_2+4\omega_1)r_1}{9\omega_2 r_2}\cos\left(\phi_2+\phi_1+\phi t_1\right)-\frac{\pi^4P_1^2}{4\omega_2}\left(2r_2^2+\sum_{l=1}^{\infty}l^2r_l^2\right)-\frac{3k_{sn}}{16\omega_2}r_1^2-\frac{k_{sl}}{2\omega_2},
\end{gathered} \tag{33}$$

From first two equations in (33); which results in that $\omega_1 r_1^2-\omega_2 r_2^2 = c_2e^{-c_dt_1}$, where c_2 is constant of integration. Now let $\Phi\left(t_1\right) = \phi_2(t_1)+\phi_1(t_1)+\phi t_1$, so from the last equation (33) it follows that:

$$\begin{gathered}
\frac{dr_1}{dt_1} = -\frac{c_d}{2}r_1+\frac{4\alpha(4\omega_1+\omega_2)}{9\omega_1}\sqrt{\frac{\omega_1r_1^2-c_1e^{-c_dt_1}}{\omega_2}}\sin(\Phi), \\
\frac{d\Phi}{dt_1} = \phi+\frac{4\alpha(4\omega_1+\omega_2)}{9}\left(\frac{\sqrt{\omega_1r_1^2-c_1e^{-c_dt_1}}}{\omega_1\sqrt{\omega_2}r_1}+\frac{r_1}{\sqrt{\omega_2}\sqrt{\omega_1r_1^2-c_1e^{-c_dt_1}}}\right)\cos(\Phi)- \\
\pi^4P_1^2\{\left(\frac{3}{32\omega_1}+\frac{1}{4\omega_2}\right)r_1^2+\left(\frac{1}{4\omega_1}+\frac{3}{2\omega_2}\right)\frac{\omega_1r_1^2-c_1e^{-c_dt_1}}{\omega_2}+ \\
\left(\frac{1}{16\omega_1}+\frac{1}{4\omega_2}\right)C^2e^{-c_dt_1}\sum_{l=3}^{\infty}l^2\}-\frac{3k_{sn}}{16\omega_2}\left(\frac{\omega_1r_1^2-c_1e^{-c_dt_1}}{\omega_1\omega_2}+\frac{r_1^2}{\omega_2}\right)-\frac{k_{sl}}{2}\left(\frac{1}{\omega_1}+\frac{1}{\omega_2}\right).
\end{gathered} \tag{34}$$

and $\dot{r}_k = -\frac{c_d}{2}r_k$ for $k = 3,4,5,\ldots.\Rightarrow r_k(t_1) = Ce^{-\frac{1}{2}c_dt_1}$.

Stability of beam in sum-type resonance of interaction first and second mode is shown by phase portraits of the system in Eq. (34) under the effect of bending stiffness P_1, nonlinear elastic foundation k_{sn} and damping c_d, while keeping other parameters fixed to 0.003. **Figure 8** shows the behaviour of the beam under the effect of bending stiffness P_1. For smaller values of P_1, as seen in **Figure 8a**, some trajectories rotate around certain fixed points, while others deviate. In **Figure 8b**, for larger values of P_1, all trajectories move away from the fixed points, leading to system instability. **Figure 9** illustrates the effects of the nonlinear elastic foundation k_{sn}. In **Figure 9a**,

for smaller values of k_{sn}, some trajectories move around the fixed points, while others deviate. However, for larger values of k_{sn}, all trajectories become unstable, as shown in **Figure 9b**. **Figure 10** presents the effects of the damping parameter c_d. In **Figure 10a**, some trajectories spiral around the fixed points, while others diverge. In **Figure 10b**, for larger values of c_d, all trajectories approach the fixed points directly, indicating that the system becomes asymptotically stable due to the stronger damping effect. So, Instability rises with larger bending stiffness P_1 and nonlinear elastic foundation k_{sn}, while stability improves with higher damping c_d.

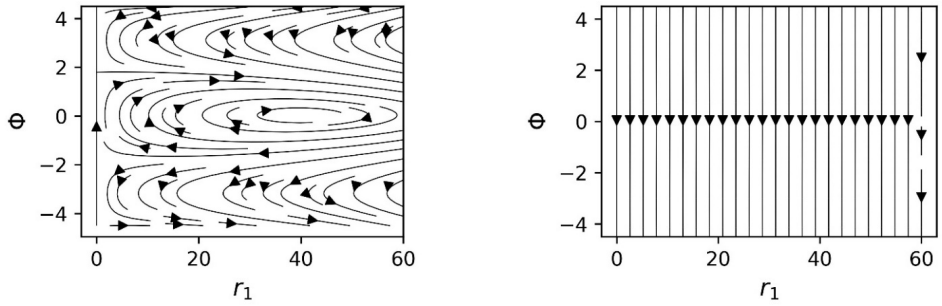

(a) **(b)**

Figure 8. Phase portraits when: **(a)** $P_1 = 0.0001$; **(b)** $P_1 = 0.1$.

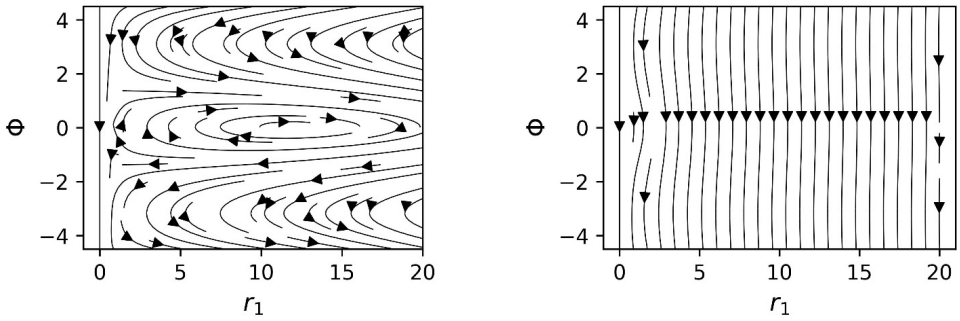

(a) **(b)**

Figure 9. Phase portraits when: **(a)** $k_{sn} = 0.0001$; **(b)** $k_{sn} = 8$.

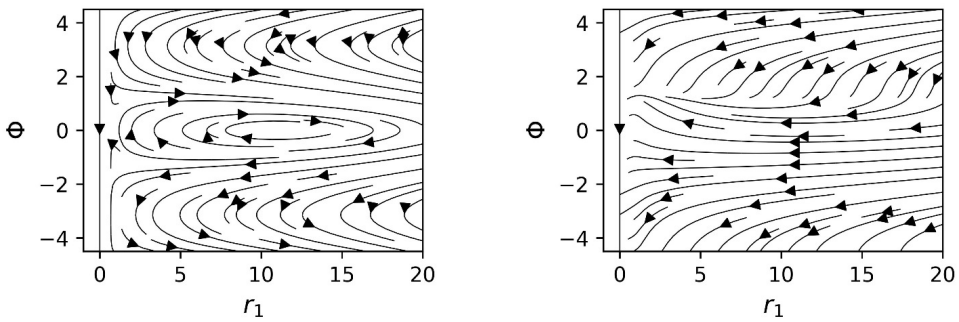

(a) **(b)**

Figure 10. Phase portraits when: **(a)** $c_d = 0.0001$; **(b)** $c_d = 0.1$.

Case 3. When $\Omega = \omega_3 - \omega_2 + \epsilon\phi$

The following coupled system is obtained in a similar way as discussed in case 1:

$$\begin{aligned}
\frac{dr_2}{dt_1} &= -\frac{c_d}{2} r_2 + \frac{12\alpha(9\omega_2 - 4\omega_3)}{25\omega_2} \sqrt{\frac{c_3 e^{-c_d t_1} - \omega_2 r_2^2}{\omega_3}} \sin(\Phi), \\
\frac{d\Phi}{dt_1} &= \phi + \frac{12\alpha(9\omega_2 - 4\omega_3)}{25} \left(\frac{\sqrt{c_3 e^{-c_d t_1} - \omega_2 r_2^2}}{\omega_2 \sqrt{\omega_3} r_2} - \frac{r_2}{\sqrt{\omega_3}\sqrt{c_3 e^{-c_d t_1} - \omega_2 r_2^2}} \right) \cos(\Phi) \\
&+ \pi^4 P_1^2 \{ 3 \left(\frac{1}{2\omega_2} - \frac{3}{4\omega_3} \right) r_2^2 + 9 \left(\frac{1}{4\omega_2} - \frac{27}{32\omega_3} \right) \frac{c_3 e^{-c_d t_1} - \omega_2 r_2^2}{\omega_3} + \\
&\left(\frac{1}{4\omega_2} - \frac{9}{16\omega_3} \right) C^2 e^{-c_d t_1} \left(1 + \sum_{l=4}^{\infty} l^2 \right) \} + \frac{3k_{sn}}{16} \left(\frac{c_3 e^{-c_d t_1} - \omega_2 r_2^2}{\omega_2 \omega_3} - \frac{r_2^2}{\omega_3} \right) + \\
&\frac{k_{sl}}{2} \left(\frac{1}{\omega_2} - \frac{1}{\omega_3} \right),
\end{aligned} \tag{35}$$

and $\dot{r}_k = -\frac{c_d}{2} r_k$ for $k = 1, 4, 5, \ldots. \Rightarrow r_k(t_1) = Ce^{-c_d t_1}$.

The interaction of the second and third modes in difference-type resonance is illustrated in **Figures 11–13** under the influence of the parameters $P_1,\ k_{sn}$ and c_d. The dynamic behavior of the beam for P_1 and c_d is like that observed in the interaction of the first and second modes in difference-type resonance. However, the instability regions appear to have significantly increased for larger values of the nonlinear elastic foundation parameter k_{sn}, indicating that stronger nonlinear elasticity is increasing the instability in this mode interaction.

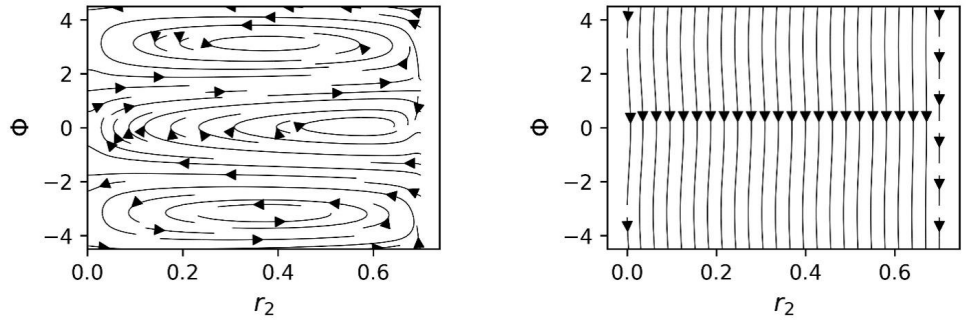

(a) **(b)**

Figure 11. Phase portraits when: **(a)** $P_1 = 0.0001$; **(b)** $P_1 = 0.1$.

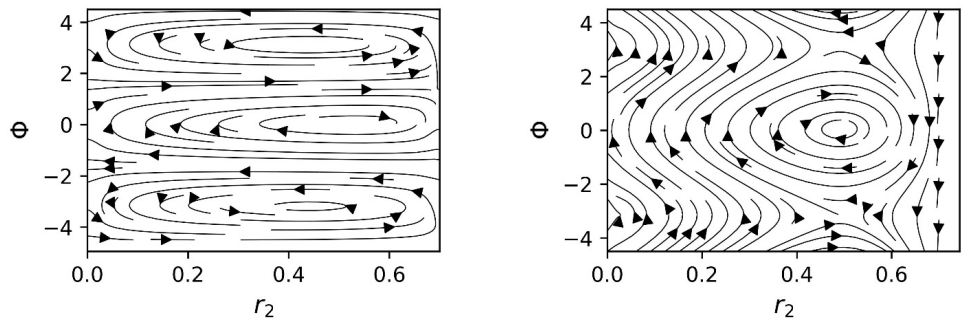

(a) **(b)**

Figure 12. Phase portraits when: **(a)** $k_{sn} = 0.0001$; **(b)** $k_{sn} = 35$.

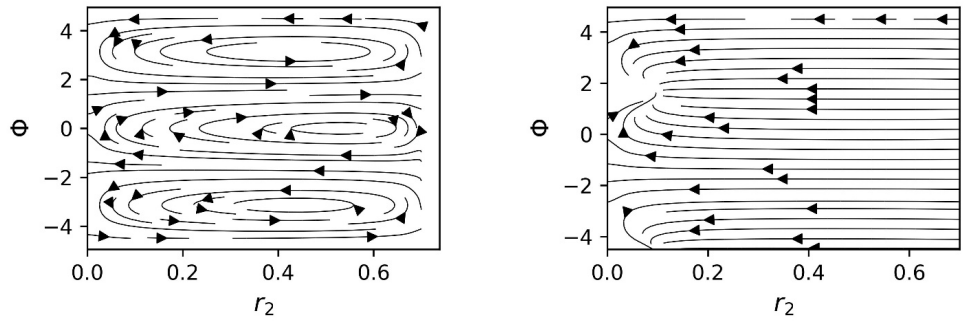

(a) **(b)**

Figure 13. Phase portraits when: **(a)** $c_d = 0.0001$: **(b)** $c_d = 0.5$.

Case 4. When $\Omega = \omega_3 + \omega_2 + \epsilon\phi$

The following coupled system is obtained in a similar way as discussed in case 2:

$$\begin{aligned}
\frac{dr_2}{dt_1} &= -\frac{c_d}{2} r_2 + \frac{12\alpha(9\omega_2+4\omega_3)}{25\omega_2}\sqrt{\frac{\omega_2 r_2^2 - c_4 e^{-c_d t_1}}{\omega_3}}\sin(\Phi),\\
\frac{d\Phi}{dt_1} &= \phi + \frac{12\alpha(9\omega_2+4\omega_3)}{25}\left(\frac{\sqrt{\omega_2 r_2^2 - c_4 e^{-c_d t_1}}}{\omega_2\sqrt{\omega_3} r_2} + \frac{r_2}{\sqrt{\omega_3}\sqrt{\omega_2 r_2^2 - c_4 e^{-c_d t_1}}}\right)\cos(\Phi)\\
&\quad -\pi^4 P_1^2\{3\left(\frac{1}{2\omega_2}+\frac{3}{4\omega_3}\right) r_2^2 + 9\left(\frac{1}{4\omega_2}+\frac{27}{32\omega_3}\right)\frac{\omega_2 r_2^2 - c_4 e^{-c_d t_1}}{\omega_3} +\\
&\quad \left(\frac{1}{4\omega_2}+\frac{9}{16\omega_3}\right) C^2 e^{-c_d t_1}\left(1+\sum_{l=4}^{\infty} l^2\right)\} - \frac{3k_{sn}}{16}\left(\frac{\omega_2 r_2^2 - c_4 e^{-c_d t_1}}{\omega_2\omega_3} + \frac{r_2^2}{\omega_3}\right)\\
&\quad -\frac{k_{sl}}{2}\left(\frac{1}{\omega_2}+\frac{1}{\omega_3}\right),
\end{aligned} \tag{36}$$

and $\dot{r}_k = -\frac{c_d}{2} r_k$ for $k = 1, 4, 5, \ldots. \Rightarrow r_k(t_1) = C$.

The interaction of the second and third modes in sum-type resonance is illustrated in **Figures 14–16** under the influence of the parameters $P_1,\ k_{sn}$ and c_d. The dynamic behavior of the beam for$P_1,\ k_{sn}$ and c_d is similar to that observed in the interaction of the first and second modes in sum-type resonance.

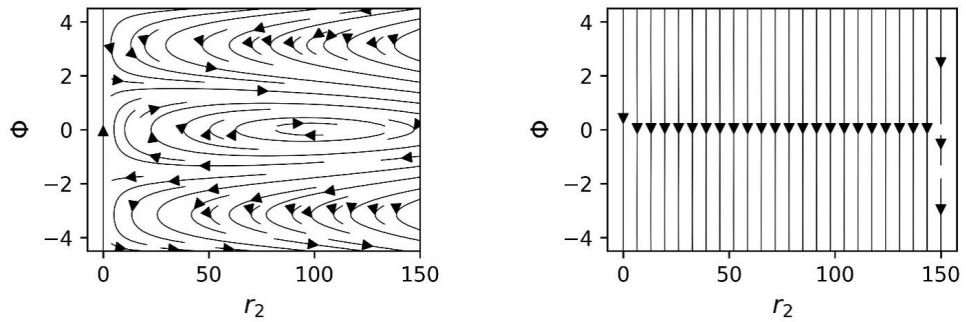

(a) **(b)**

Figure 14. Phase portraits when: **(a)** $P_1 = 0.0001$; **(b)** $P_1 = 0.1$.

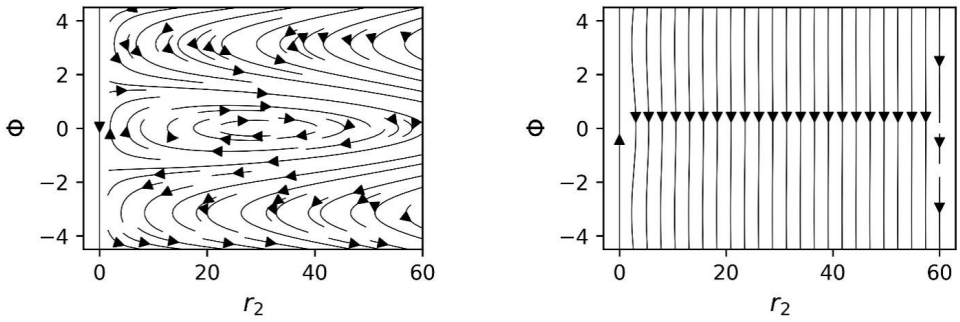

(a) **(b)**

Figure 15. Phase portraits when: **(a)** $k_{sn} = 0.0001$; **(b)** $k_{sn} = 35$.

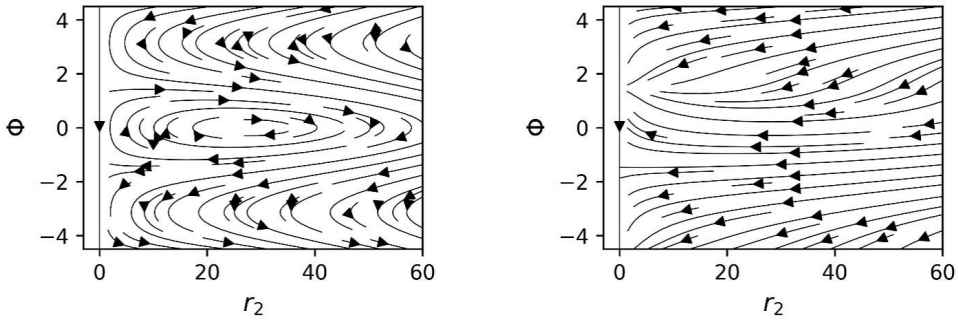

(a) **(b)**

Figure 16. Phase portraits when: **(a)** $c_d = 0.0001$; **(b)** $c_d = 0.5$.

5. Conclusion

The stability of nonlinear dynamics of an axially moving damped beam on a nonlinear elastic foundation is examined. Mathematically, the nonlinear transverse vibrations of the system are formulated as fourth order nonlinear homogeneous partial differential equations (PDE) with variable coefficients. The PDE is discretized by using Fourier Expansion method into infinite dimensional system of coupled ordinary differential equations and then resulting equations are handled by two-timescales perturbation method to analyze the fast and slow dynamics in the system. It is found that the system exhibits infinitely many resonances, characterized by condition $\Omega = \pm\omega_n \pm \omega_k$. This implies that resonance occurs when frequency Ω matches the sum difference of the natural frequencies ω_n and ω_k, leading to multiple resonant interactions across the system. In this work, the stability of the system is examined in the following cases:

i. Non-resonant case:
   $\Omega \neq \pm\omega_n \pm \omega_k$
ii. Difference-type resonance:
   $\Omega = \omega_2 - \omega_1 + \epsilon\phi$, and $\Omega = \omega_3 - \omega_2 + \epsilon\phi$
iii. Sum-type resonance:
   $\Omega = \omega_2 + \omega_1 + \epsilon\phi$, and $\Omega = \omega_3 + \omega_2 + \epsilon\phi$

In the non-resonant case, the effects of bending stiffness, nonlinear elastic

foundation, and damping were analysed. It was observed that for smaller values of bending stiffness and nonlinear elastic foundation, the system exhibits an asymptotically stable solution, indicating that all trajectories eventually settle at equilibrium. However, for larger values of bending stiffness and nonlinear elastic foundation, periodic solutions arise, meaning that the system sustains oscillations around certain points. Additionally, for smaller values of damping, the system remains oscillatory, whereas for larger values of damping, all trajectories converge asymptotically to the origin, demonstrating that increased damping enhances energy dissipation and stabilizes the system.

In difference-type resonance, it was observed that for smaller values of bending stiffness, the system exhibits oscillatory solutions, while for larger values of bending stiffness, the system becomes unstable, with trajectories diverging over time. For smaller values of the nonlinear elastic foundation, the system undergoes periodic oscillations, whereas for relatively larger values, the instability region increases, indicating that stronger nonlinearity contributes to system divergence. Similarly, for smaller values of damping, the system yields periodic solutions, but for larger values, the system becomes asymptotically stable, showing that damping suppresses oscillations and stabilizes the response.

In sum-type resonance, for smaller values of bending stiffness, the system exhibits a mix of bounded and unstable solutions, while for larger values of bending stiffness, the system becomes completely unstable, with all trajectories diverging. For smaller values of the nonlinear elastic foundation, the system exhibits both periodic oscillations and some unstable solutions, whereas for relatively larger values, the system becomes entirely unstable. Regarding damping, for smaller values, the system displays both periodic and unstable solutions, while for larger values, the solutions become asymptotically stable, confirming that increased damping mitigates instability and ensures convergence toward equilibrium.

Comparing resonant and non-resonant regimes, resonant cases exhibit wider instability regions and are far more sensitive to nonlinear foundation effects, underlining their importance in engineering design considerations. The present analysis is restricted to the small-parameter assumption $\epsilon \ll 1$, which acts as a bookkeeping device representing the smallness of damping, foundation, and nonlinear effects, which justifies the use of the two-timescale method in the weakly nonlinear regime considered here. Nevertheless, harmonic axial speed can lead to internal and parametric resonances that require careful treatment. For regimes where the smallness assumption is less justified, alternative perturbation strategies such as the homotopy perturbation method (HPM) may provide complementary insights, particularly in capturing moderate nonlinearities or additional solution branches. Future work should extend to stronger nonlinearities, alternative foundation models, external excitations, and systematic numerical comparisons. Furthermore, the validity of the results is confirmed in **Appendix C**. In the limiting case when damping and foundation effects are neglected, the system reduces exactly to that given by Suweken and Van Horssen [41], and the corresponding phase portraits are in full agreement.

Author contributions: Conceptualization, G.Y.M. and R.A.M.; methodology, M.M.; software, M.B.A.; validation, I.A.A.; formal analysis, R.A.M.; investigation, G.Y.M.; writing—original draft preparation, G.Y.M.; writing—review and editing, G.Y.M. and M.M.; visualization, M.B.A. and I.A.A.; supervision, R.A.M. All authors have read and agreed to the published version of the manuscript.

Data availability statement: Data sharing is not applicable to this article, as all the data used to obtain the results is included within the article.

Conflict of interest: The authors declare no conflicts of interest.

References

1. Wang KW, Mote CD. Vibration coupling analysis of band/wheel mechanical systems. Journal of Sound and Vibration. 1986; 109(2): 237–258. doi: 10.1016/S0022-460X(86)80006-2
2. Pham PT, Hong KS. Dynamic models of axially moving systems: A review. Nonlinear Dynamics. 2020; 100(1): 315–349. doi: 10.1007/s11071-020-05491-z
3. Hamidi BA, Hosseini SA, Hayati H, et al. Forced axial vibration of micro and nanobeam under axial harmonic moving and constant distributed forces via nonlocal strain gradient theory. Mechanics Based Design of Structures and Machines. 2022; 50(5): 1491–1505. doi: 10.1080/15397734.2020.1744003
4. Zhu WD, Ren H, Xiao C. A nonlinear model of a slack cable with bending stiffness and moving ends with application to elevator traveling and compensation cables. Journal of Applied Mechanics, Transactions ASME. 2011; 78(4): 41017.
5. Öz HR, Boyaci H. Transverse vibrations of tensioned pipes conveying fluid with time-dependent velocity. Journal of Sound and Vibration. 2000; 236(2): 259–76. doi: 10.1006/jsvi.2000.2985
6. Sandilo SH, Van Horssen WT. On boundary damping for an axially moving tensioned beam. Journal of vibration and acoustics. 2012; 134(1): 011005. doi: 10.1115/1.4005025
7. Malookani RA, Van Horssen WT. On the asymptotic approximation of the solution of an equation for a non-constant axially moving string. Journal of Sound and Vibration. 2016; 367: 203–218. doi: 10.1016/j.jsv.2015.12.043
8. Ghayesh MH, Amabili M, Païdoussis MP. Nonlinear vibrations and stability of an axially moving beam with an intermediate spring support: two-dimensional analysis. Nonlinear Dynamics. 2012; 70(1): 335–354. doi: 10.1007/s11071-012-0458-3
9. Pellicano F, Mastroddi F. Nonlinear dynamics of a beam on elastic foundation. Nonlinear Dynamics. 1997; 14(4): 335–355. doi: 10.1023/A:1008297721253
10. Öz HR, Pakdemirli M, Özkaya E, et al. Non-linear vibrations of a slightly curved beam resting on a non-linear elastic foundation. Journal of Sound and Vibration. 1998; 212(2): 295–309. doi: 10.1006/jsvi.1997.1428
11. Ghayesh MH. Nonlinear dynamic response of a simply-supported Kelvin–Voigt viscoelastic beam, additionally supported by a nonlinear spring. Nonlinear Analysis: Real World Applications. 2012; 13(3): 1319–1333. doi: 10.1016/j.nonrwa.2011.10.009
12. Ali S, Khan S, Jamal A, et al. Transverse response of an axially moving beam with intermediate viscoelastic support. Mathematical Problems in Engineering. 2021; 2021: 1–14. doi: 10.1155/2021/2218832
13. Li YH, Wang L, Yang EC. Nonlinear dynamic responses of an axially moving laminated beam subjected to both blast and thermal loads. International Journal of Non-Linear Mechanics. 2018; 101: 56–67. doi: 10.1016/j.ijnonlinmec.2018.02.007
14. Amer YA, EL-Sayed AT, Abd EL-Salam MN. A suitable active control for suppression the vibrations of a cantilever beam. Sound&Vibration. 2022; 56(2): 89–104. doi: 10.32604/sv.2022.011838
15. Çuvalcı O, Ünker F, Batuhan Baturalp T, et al. Modal control of cantilever beam using a gyrostabilizer. Sound&Vibration. 2021; 55(4): 281–94. doi: 10.32604/sv.2021.015705
16. Yang Y, Wang Z. Transverse vibration and stability analysis of circular plate subjected to follower force and thermal load. Sound&Vibration. 2019; 53(3): 51–64. doi: 10.32604/sv.2019.04004
17. Xu D, Du J, Zhao Y. Flexural vibration and power flow analyses of axially loaded beams with general boundary and non-uniform elastic foundations. Advances in Mechanical Engineering. 2020; 12(5): 1687814020921719. doi: 10.1177/1687814020921719

18. Mamandi A. Vibration control of an axially loaded composite beam bonded with Piezoelectric actuator and sensor layers on a Winkler–Pasternak foundation and under transverse excitation force based on first-order shear deformation theory. Sādhanā. 2023; 48(4): 191. doi: 10.1007/s12046-023-02239-4
19. Li C, Cheng Y, O'Regan D. High-gain stabilization for an axially moving beam under boundary feedback control. Mathematical Methods in the Applied Sciences. 2023; 46(2): 1789–1808. doi: 10.1002/mma.8609
20. Sheng GG, Han Y, Zhang Z, et al. Control of nonlinear vibration of beams subjected to moving loads using tuned mass dampers. Acta Mechanica. 2023; 234(7): 3019–3036. doi: 10.1007/s00707-023-03544-z
21. Zhou J, Quan X, Mou H, et al. Post-buckling behavior of axially moving beams under external loads and nonlinear vibration characterization. Journal of Vibration Engineering & Technologies. 2025; 13(1): 67. doi: 10.1007/s42417-024-01606-7
22. Fang X, Huang L, Lou Z, et al. Quasi-periodic and periodic vibration responses of an axially moving beam under multiple-frequency excitation. Mathematics. 2024; 12(17): 2608. doi: 10.3390/math12172608
23. Abramian AK, Vakulenko SA, van Horssen WT. On the existence and approximation of localized waves in a damped Euler-Bernoulli beam on a nonlinear elastic foundation. Nonlinear Dynamics. 2025; 113(19): 26561-26581.
24. Liu M, Yao G. Nonlinear forced vibration and stability of an axially moving beam with a free internal hinge. Nonlinear Dynamics. 2024; 112(9): 6877–6896. doi: 10.1007/s11071-024-09447-5
25. Zhai YJ, Ma ZS, Ding Q, et al. Nonlinear transverse vibrations of a slightly curved beam with hinged–hinged boundaries subject to axial loads. Archive of Applied Mechanics. 2022; 92(7): 2081–94. doi: 10.1007/s00419-022-02162-w
26. Kang H, Wang Y, Zhao Y. Nonlinear vibration analysis of a double-cable beam structure with nonlinear energy sinks. Communications in Nonlinear Science and Numerical Simulation. 2025; 142: 108529. doi: 10.1016/j.cnsns.2024.108529
27. Zamani HA, Nourazar SS, Aghdam MM. Large-amplitude vibration and buckling analysis of foam beams on nonlinear elastic foundations. Mechanics of Time-Dependent Materials. 2024; 28(2): 363–380. doi: 10.1007/s11043-022-09568-7
28. Jiang J, Lian C, Meng B, et al. An approximate solution of the bending of beams on a nonlinear elastic foundation with the galerkin method. Journal of Applied and Computational Mechanics. 2024; (Online First). doi: 10.22055/jacm.2024.46952.4633
29. Mallah GY, Malookani RA, Sandilo SH, et al. On Stability Analysis of Linear Axially Moving Damped Beam with Elastic Foundation. International Journal of Differential Equations. 2024; 2024(1): 8893138. doi: 10.1155/2024/8893138
30. Hu H. A classical perturbation technique which is valid for large parameters. Journal of Sound and Vibration. 2004; 269(1–2): 409–412. doi: 10.1016/S0022-460X(03)00318-3
31. Xiao-dong Y, Li-qun C. Dynamic stability of axially moving viscoelastic beams with pulsating speed. Applied Mathematics and Mechanics. 2005; 26(8): 989–995. doi: 10.1007/BF02466411
32. Chen LQ, Wang B. Stability of axially accelerating viscoelastic beams: asymptotic perturbation analysis and differential quadrature validation. European Journal of Mechanics: A/Solids. 2009; 28(4): 786–791. doi: 10.1016/j.euromechsol.2008.12.002
33. Ding H, Chen L. On two transverse nonlinear models of axially moving beams. Science in China Series E: Technological Sciences. 2009; 52(3): 743–751. doi: 10.1007/s11431-009-0060-1
34. Yang XD, Chen LQ. Dynamic stability of an axially accelerating viscoelastic beam with two fixed supports. International Journal of Structural Stability and Dynamics. 2006; 06(01): 31–42. doi: 10.1142/S0219455406001812
35. Yang XD, Lim CW, Liew KM. Vibration and stability of an axially moving beam on elastic foundation. Advances in Structural Engineering. 2010; 13(2): 241–247. doi: 10.1260/1369-4332.13.2.241
36. Norouzi H, Younesian D. Chaotic vibrations of beams on nonlinear elastic foundations subjected to reciprocating loads. Mechanics Research Communications. 2015; 69: 121–128. doi: 10.1016/j.mechrescom.2015.07.001
37. Mirzabeigy A, Madoliat R. Large amplitude free vibration of axially loaded beams resting on variable elastic foundation. Alexandria Engineering Journal. 2016; 55(2): 1107–1114. doi: 10.1016/j.aej.2016.03.021
38. El-Dib YO, Elgazery NS. Damped mathieu equation with a modulation property of the homotopy perturbation method. Sound&Vibration. 2022; 56(1): 21–36. doi: 10.32604/sv.2022.014166
39. Fatih KMM, Mehmet P. Vibration analysis of a beam on a nonlinear elastic foundation. Structural Engineering and Mechanics. 2017; 62(2): 171–178. doi: 10.12989/SEM.2017.62.2.171
40. Alimoradzadeh M, Salehi M, Esfarjani SM. Nonlinear dynamic response of an axially functionally graded (afg) beam

resting on nonlinear elastic foundation subjected to moving load. Nonlinear Engineering. 2019; 8(1): 250–60. doi: 10.1515/nleng-2018-0051
41. Suweken G, Van Horssen WT. On the weakly nonlinear, transversal vibrations of a conveyor belt with a low and time-varying velocity. Nonlinear Dynamics. 2003; 31(2): 197–223. doi: 10.1023/A:1022053131286
42. Zhang DB, Tang YQ, Liang RQ, et al. Dynamic stability of an axially transporting beam with two-frequency parametric excitation and internal resonance. European Journal of Mechanics - A/Solids. 2021; 85: 104084. doi: 10.1016/j.euromechsol.2020.104084

Appendix A

In this appendix, it is shown that when $\Omega = \omega_2 \pm \omega_1$, if $k = 1$, $n = 2$ then $p = 1$, $q = 2$ and if $k = 2$, $n = 1$ then $p = 2$, $q = 1$. The secular terms will arise for non-linear elastic foundation in Eq. (25), if $\pm\omega_k = \pm\omega_n \pm \omega_p \pm \omega_q$, where $k = n + p + q$ or $k = -n - p + q$ or $k = n + p - q$ with k, n, p, $q \in \mathbb{N}^+$. So, the following cases will be considered:

(a) $k\left(1+\mu^2k^2\right)^{\frac{1}{2}} = n\left(1+\mu^2n^2\right)^{\frac{1}{2}} + p\left(1+\mu^2p^2\right)^{\frac{1}{2}} + q\left(1+\mu^2q^2\right)^{\frac{1}{2}}$
For $k = 1$, $n = 2$ and $k = 2$, $n = 1$, there is not any solution for p,$q \geq 1$.

(b) $k\left(1+\mu^2k^2\right)^{\frac{1}{2}} = -n\left(1+\mu^2n^2\right)^{\frac{1}{2}} - p\left(1+\mu^2p^2\right)^{\frac{1}{2}} - q\left(1+\mu^2q^2\right)^{\frac{1}{2}}$
For $k = 1$, $n = 2$ and $k = 2$, $n = 1$, there is not any solution for p,$q \geq 1$

(c) $k\left(1+\mu^2k^2\right)^{\frac{1}{2}} = n\left(1+\mu^2n^2\right)^{\frac{1}{2}} + p\left(1+\mu^2p^2\right)^{\frac{1}{2}} - q\left(1+\mu^2q^2\right)^{\frac{1}{2}}$
When $k = 1$ and $n = 2$, it has solution if $p = 1$ and $q = 2$ and when $k = 2$ and $n = 1$, it has solution if $p = 2$ and $q = 1$.

(d) $k\left(1+\mu^2k^2\right)^{\frac{1}{2}} = n\left(1+\mu^2n^2\right)^{\frac{1}{2}} - p\left(1+\mu^2p^2\right)^{\frac{1}{2}} + q\left(1+\mu^2q^2\right)^{\frac{1}{2}}$
When $k = 1$ and $n = 2$, it has solution if $p = 2$ and $q = 1$ and when $k = 2$ and $n = 1$, it has solution if $p = 1$ and $q = 2$.

(e) $k\left(1+\mu^2k^2\right)^{\frac{1}{2}} = -n\left(1+\mu^2n^2\right)^{\frac{1}{2}} + p\left(1+\mu^2p^2\right)^{\frac{1}{2}} + q\left(1+\mu^2q^2\right)^{\frac{1}{2}}$
When $k = 1$ and $n = 2$, it has solution if $p = 1$ and $q = 2$ or $p = 2$ and $q = 1$ and when $k = 2$ and $n = 1$, it has solution if $p = 1$ and $q = 2$ or $p = 2$ and $q = 1$.

(f) $\left(1+\mu^2k^2\right)^{\frac{1}{2}} = -n\left(1+\mu^2n^2\right)^{\frac{1}{2}} - p\left(1+\mu^2p^2\right)^{\frac{1}{2}} + q\left(1+\mu^2q^2\right)^{\frac{1}{2}}$
For $k = 1$, $n = 2$ and $k = 2$, $n = 1$, there is not any solution for p,$q \geq 1$.

(g) $\left(1+\mu^2k^2\right)^{\frac{1}{2}} = -n\left(1+\mu^2n^2\right)^{\frac{1}{2}} + p\left(1+\mu^2p^2\right)^{\frac{1}{2}} - q\left(1+\mu^2q^2\right)^{\frac{1}{2}}$
For $k = 1$, $n = 2$ and $k = 2$, $n = 1$, there is not any solution for p,$q \geq 1$.

(h) $\left(1+\mu^2k^2\right)^{\frac{1}{2}} = n\left(1+\mu^2n^2\right)^{\frac{1}{2}} - p\left(1+\mu^2p^2\right)^{\frac{1}{2}} - q\left(1+\mu^2q^2\right)^{\frac{1}{2}}$
For $k = 1$, $n = 2$ and $k = 2$, $n = 1$, there is not any solution for p,$q \geq 1$.

So, only possible solution from above which satisfy $k = n + p + q$ or$k = -n - p + q$ or$k = n + p - q$ is in case (c) and case (e), that is when if $k = 1$, $n = 2$ then $p = 1$, $q = 2$ and if $k = 2$,$n = 1$ then $p = 2$,$q = 1$ because it will also hold for $k = n + p - q$.

Appendix B

In this appendix, the derivation of coupled system of ODEs (29) is discussed in detail and it is shown that how the secular terms are eliminated in Eq. (25).

When $\Omega = \omega_2 - \omega_1 + \epsilon\phi$ for $k = 1$ and $n = 2$, substituting in Eq. (25) yields:

$$\begin{gathered}
\frac{\partial^2 v_{11}}{\partial t_0^2} + \omega_1^2 v_{11} = -2\omega_1 \left(\frac{dA_{10}}{dt_1} \cos(\omega_1 t_0) - \frac{dB_{10}}{dt_1} \sin(\omega_1 t_0) \right) + \left[\sum_{j=0} - \sum_{j=-1} - \sum_{j=1} \right] \frac{4\alpha\omega_2}{(2j+1)} \\
[A_{20} \{ \sin(2\omega_2 - \omega_1 + \epsilon\phi) t_0 + \sin(-\omega_1 + \epsilon\phi) t_0 \} - B_{20} \{ \cos(-\omega_1 + \epsilon\phi) t_0 - \\
\cos(2\omega_2 - \omega_1 + \epsilon\phi) t_0 \}] + \left[\sum_{j=0} + \sum_{j=-1} - \sum_{j=1} \right] \frac{4\alpha(\omega_2 - \omega_1 + \epsilon\phi)}{(2j+1)^2} \\
[A_{20} \{ \sin(2\omega_2 - \omega_1 + \epsilon\phi) t_0 - \sin(-\omega_1 + \epsilon\phi) t_0 \} + B_{20} \{ \cos(-\omega_1 + \epsilon\phi) t_0 + \cos(2\omega_2 - \omega_1 + \epsilon\phi) t_0 \}] \\
-\frac{3k_{sn}}{16} [A_{20} A_{10} B_{20} \{ \cos(2\omega_2 - \omega_1) t_0 + \cos(-\omega_1) t_0 - \cos(2\omega_2 + \omega_1) t_0 - \cos(\omega_1) t_0 \} + \\
A_{20}^2 B_{10} \{ \cos(\omega_1) t_0 - \cos(2\omega_2 + \omega_1) t_0 + \cos(-\omega_1) t_0 - \cos(2\omega_2 - \omega_1) t_0 \} + \\
B_{20} A_{10} A_{20} \{ \cos(\omega_1) t_0 - \cos(2\omega_2 + \omega_1) t_0 - \cos(-\omega_1) t_0 + \cos(2\omega_2 - \omega_1) t_0 \} + \\
B_{20}^2 B_{10} \{ \cos(2\omega_2 + \omega_1) t_0 + \cos(\omega_1) t_0 + \cos(2\omega_2 - \omega_1) t_0 + \cos(-\omega_1) t_0 \} + \\
A_{20}^2 A_{10} \{ \sin(2\omega_2 - \omega_1) t_0 - \sin(-\omega_1) t_0 - \sin(2\omega_2 + \omega_1) t_0 + \sin(\omega_1) t_0 \} + \\
A_{20} B_{10} B_{20} \{ \sin(2\omega_2 + \omega_1) t_0 + \sin(\omega_1) t_0 + \sin(2\omega_2 - \omega_1) t_0 + \sin(-\omega_1) t_0 \} + \\
B_{20}^2 A_{10} \{ \sin(2\omega_2 + \omega_1) t_0 + \sin(\omega_1) t_0 - \sin(2\omega_2 - \omega_1) t_0 - \sin(-\omega_1) t_0 \} + \\
B_{20} B_{10} A_{20} \{ \sin(2\omega_2 + \omega_1) t_0 - \sin(\omega_1) t_0 + \sin(2\omega_2 - \omega_1) t_0 - \sin(-\omega_1) t_0 \}] - \\
\frac{\pi^4 P_1^2}{8} \{ A_{10} \sin(\omega_1) t_0 + B_{10} \cos(\omega_1) t_0 \} \sum_{l=1}^{\infty} l^2 \left(A_{l0}^2 + B_{l0}^2 \right) - \frac{\pi^4 P_1^2}{16} \left(B_{10}^2 - A_{10}^2 \right) \\
[A_{10} \{ \sin(3\omega_1) t_0 - \sin(\omega_1) t_0 \} + B_{10} \{ \cos(3\omega_1) t_0 + \cos(\omega_1) t_0 \}] - \\
\frac{\pi^4 P_1^2}{8} A_{10} B_{10} [A_{10} \{ \cos(\omega_1) t_0 - \cos(3\omega_1) t_0 \} + B_{10} \{ \sin(3\omega_1) t_0 + \sin(\omega_1) t_0 \}] \\
-k_{sl} (A_{10}(t_1) \sin(\omega_1 t_0) + B_{10}(t_1) \cos(\omega_1 t_0)) - c_d \omega_1 (A_{10} \cos(\omega_1 t_0) - B_{10} \sin(\omega_1 t_0)) \\
+\text{Non Secular Terms},
\end{gathered} \tag{A1}$$

Simplifying and making the terms on the right side of Eq. (A1) equal to zero, which generate resonances, it follows that:

$$\begin{gathered}
-2\omega_1 \left(\frac{dA_{10}}{dt_1} \cos(\omega_1 t_0) - \frac{dB_{10}}{dt_1} \sin(\omega_1 t_0) \right) + \left(1 - \tfrac{1}{3}\right) 4\alpha\omega_2 [A_{20} \{ \sin(\phi t_1) \cos(\omega_1 t_0) - \cos(\phi t_1) \sin(\omega_1 t_0) \} \\
-B_{20} \{ \cos(\phi t_1) \cos(\omega_1 t_0) + \sin(\phi t_1) \sin(\omega_1 t_0) \}] + \left(1 - \tfrac{1}{9}\right) 4\alpha (\omega_2 - \omega_1) [A_{20} \{ \cos(\phi t_1) \sin(\omega_1 t_0) - \\
\sin(\phi t_1) \cos(\omega_1 t_0) \} + B_{20} \{ \cos(\phi t_1) \cos(\omega_1 t_0) + \sin(\phi t_1) \sin(\omega_1 t_0) \}] - \frac{3k_{sn}}{16} [\{ 2A_{20}^2 B_{10} \cos(\omega_1) t_0 \} \\
+ \{ 2B_{20}^2 B_{10} \cos(\omega_1) t_0 \} + \{ 2A_{20}^2 A_{10} \sin(\omega_1) t_0 \} + \{ 2B_{20}^2 A_{10} \sin(\omega_1) t_0 \}] - \\
\frac{\pi^4 P_1^2}{8} \{ A_{10} \sin(\omega_1) t_0 + B_{10} \cos(\omega_1) t_0 \} \sum_{l=1}^{\infty} l^2 \left(A_{l0}^2 + B_{l0}^2 \right) - \frac{\pi^4 P_1^2}{16} \left(B_{10}^2 - A_{10}^2 \right) \{ -A_{10} \sin(\omega_1) t_0 \\
+B_{10} \cos(\omega_1) t_0 \} - \frac{\pi^4 P_1^2}{8} A_{10} B_{10} \{ A_{10} \cos(\omega_1) t_0 + B_{10} \sin(\omega_1) t_0 \} - k_{sl} \{ A_{10} \sin(\omega_1 t_0) + \\
B_{10} \cos(\omega_1 t_0) \} - c_d \omega_1 \{ A_{10} \cos(\omega_1 t_0) - B_{10} \sin(\omega_1 t_0) \} = 0,
\end{gathered} \tag{A2}$$

Equating the coefficients of $\cos(\omega_1 t_0)$ and $\sin(\omega_1 t_0)$ in Eq. (A2) respectively and simplifying, the following equations are obtained:

$$\begin{gathered}
\frac{dA_{10}}{dt_1} = -\frac{4\alpha}{9\omega_1} (\omega_2 - 4\omega_1) A_{20} \sin(\phi t_1) + \frac{4\alpha}{9\omega_1} (\omega_2 - 4\omega_1) B_{20} \cos(\phi t_1) - \frac{\pi^4 P_1^2}{32\omega_1} B_{10} \{ \left(A_{10}^2 + B_{10}^2 \right) + \\
2 \sum_{l=1}^{\infty} l^2 \left(A_{l0}^2 + B_{l0}^2 \right) \} - \frac{3k_{sn}}{16\omega_1} \left(A_{20}^2 + B_{20}^2 \right) B_{10} - \frac{k_{sl}}{2\omega_1} B_{10} - \frac{c_d}{2} A_{10}, \\
\frac{dB_{10}}{dt_1} = -\frac{4\alpha}{9\omega_1} (\omega_2 - 4\omega_1) A_{20} \cos(\phi t_1) - \frac{4\alpha}{9\omega_1} (\omega_2 - 4\omega_1) B_{20} \sin(\phi t_1) + \frac{\pi^4 P_1^2}{32\omega_1} A_{10} \{ \left(A_{10}^2 + B_{10}^2 \right) \\
+2 \sum_{l=1}^{\infty} l^2 \left(A_{l0}^2 + B_{l0}^2 \right) \} + \frac{3k_{sn}}{16\omega_1} \left(A_{20}^2 + B_{20}^2 \right) A_{10} + \frac{k_{sl}}{2\omega_1} A_{10} - \frac{c_d}{2} B_{10}.
\end{gathered} \tag{A3}$$

When $\Omega = \omega_2 - \omega_1 + \epsilon\phi$ for $k = 2$ and $n = 1$, substituting in Eq. (25) yields:

$$\begin{gathered}\frac{\partial^2 v_{21}}{\partial t_0^2} + \omega_2^2 v_{21} = -2\omega_2\left(\frac{dA_{20}}{dt_1}\cos(\omega_2 t_0) - \frac{dB_{20}}{dt_1}\sin(\omega_2 t_0)\right) + \left[\sum_{j=-1} - \sum_{j=0} - \sum_{j=1}\right]\frac{2\alpha\omega_1}{(2j+1)} \\ [A_{10}\{\sin(\omega_2+\epsilon\phi)t_0 + \sin(\omega_2 - 2\omega_1 + \epsilon\phi)t_0\} - B_{10}\{\cos(\omega_2 - 2\omega_1 + \epsilon\phi)t_0 - \cos(\omega_2+\epsilon\phi)t_0\}] \\ + \left[\sum_{j=-1} + \sum_{j=0} - \sum_{j=1}\right]\frac{\alpha(\omega_2-\omega_1+\epsilon\phi)}{(2j+1)^2}[A_{10}\{\sin(\omega_2+\epsilon\phi)t_0 - \sin(\omega_2 - 2\omega_1+\epsilon\phi)t_0\} + \\ B_{10}\{\cos(\omega_2 - 2\omega_1+\epsilon\phi)t_0 + \cos(\omega_2+\epsilon\phi)t_0\}]\frac{3k_{sn}}{16}[A_{10}A_{20}B_{10}\{\cos(2\omega_1-\omega_2)t_0 + \cos(-\omega_2)t_0 - \\ \cos(2\omega_1+\omega_2)t_0 - \cos(\omega_2)t_0\} + A_{10}^2 B_{20}\{\cos(\omega_1)t_0 - \cos(2\omega_1+\omega_2)t_0 + \cos(-\omega_2)t_0 - \cos(2\omega_1-\omega_2)t_0\} \\ + B_{10}A_{20}A_{10}\{\cos(\omega_2)t_0 - \cos(2\omega_1+\omega_2)t_0 - \cos(-\omega_2)t_0 + \cos(2\omega_1-\omega_2)t_0\} + \\ B_{10}^2 B_{20}\{\cos(2\omega_1+\omega_2)t_0 + \cos(\omega_2)t_0 + \cos(2\omega_1-\omega_2)t_0 + \cos(-\omega_2)t_0\} + \\ A_{10}^2 A_{20}\{\sin(2\omega_1-\omega_2)t_0 - \sin(-\omega_2)t_0 - \sin(2\omega_1+\omega_2)t_0 + \sin(\omega_2)t_0\} + \\ A_{10}B_{20}B_{10}\{\sin(2\omega_1+\omega_2)t_0 + \sin(\omega_2)t_0 + \sin(2\omega_1-\omega_2)t_0 + \sin(-\omega_2)t_0\} + \\ B_{10}^2 A_{20}\{\sin(2\omega_1+\omega_2)t_0 + \sin(\omega_2)t_0 - \sin(2\omega_1-\omega_2)t_0 - \sin(-\omega_2)t_0\} + \\ B_{10}B_{20}A_{10}\{\sin(2\omega_1+\omega_2)t_0 - \sin(\omega_2)t_0 + \sin(2\omega_1-\omega_2)t_0 - \sin(-\omega_2)t_0\}] - \\ \frac{\pi^4 P_1^2}{2}\{A_{20}\sin(\omega_2)t_0 + B_{20}\cos(\omega_2)t_0\}\sum_{l=1}^{\infty} l^2\left(A_{l0}^2 + B_{l0}^2\right) - \frac{\pi^4 P_1^2}{4}4\left(B_{20}^2 - A_{20}^2\right) \\ [A_{20}\{\sin(3\omega_2)t_0 - \sin(\omega_2)t_0\} + B_{20}\{\cos(3\omega_2)t_0 + \cos(\omega_2)t_0\}] - \frac{\pi^4 P_1^2}{2}4A_{20}B_{20}[A_{20}\{\cos(\omega_2)t_0 \\ - \cos(3\omega_2)t_0\} + B_{20}\{\sin(3\omega_2)t_0 + \sin(\omega_2)t_0\}] - k_{sl}\{A_{20}\sin(\omega_2 t_0) + B_{20}\cos(\omega_2 t_0)\} - \\ c_d\omega_2\{A_{20}\cos(\omega_2 t_0) - B_{20}\sin(\omega_2 t_0)\} + \text{Non Secular Terms},\end{gathered} \tag{A4}$$

Simplifying and making the terms on the right side of Eq. (A4) equal to zero, which generate resonances, it follows that:

$$\begin{gathered}-2\omega_2\left(\frac{dA_{20}}{dt_1}\cos(\omega_2 t_0) - \frac{dB_{20}}{dt_1}\sin(\omega_2 t_0)\right) + \left(-1 - \tfrac{1}{3}\right)2\alpha\omega_1[A_{10}\{\sin(\phi t_1)\cos(\omega_2 t_0) + \cos(\phi t_1)\sin(\omega_2 t_0)\} + \\ B_{10}\{\cos(\phi t_1)\cos(\omega_2 t_0) - \sin(\phi t_1)\sin(\omega_2 t_0)\}] + \left(1 - \tfrac{1}{9}\right)\alpha(\omega_2 - \omega_1)[A_{10}\{\cos(\phi t_1)\sin(\omega_2 t_0) + \\ \sin(\phi t_1)\cos(\omega_2 t_0)\} + B_{10}\{\cos(\phi t_1)\cos(\omega_2 t_0) - \sin(\phi t_1)\sin(\omega_2 t_0)\}] - \frac{3k_{sn}}{16}[\left\{2A_{10}^2 B_{20}\cos(\omega_2)t_0\right\} + \\ \left\{2B_{10}^2 B_{20}\cos(\omega_2)t_0\right\} + \left\{2A_{10}^2 A_{20}\sin(\omega_2)t_0\right\} + \left\{2B_{10}^2 A_{20}\sin(\omega_2)t_0\right\}] - \\ \frac{\pi^4 P_1^2}{2}\{A_{20}\sin(\omega_2)t_0 + B_{20}\cos(\omega_2)t_0\}\sum_{l=1}^{\infty} l^2\left(A_{l0}^2 + B_{l0}^2\right) - \pi^4 P_1^2\left(B_{20}^2 - A_{20}^2\right)\{-A_{20}\sin(\omega_2)t_0 + \\ B_{20}\cos(\omega_2)t_0\} - 2\pi^4 P_1^2 A_{20}B_{20}\{A_{20}\cos(\omega_2)t_0 + B_{20}\sin(\omega_2)t_0\} - k_{sl}\{A_{20}\sin(\omega_2 t_0) + \\ B_{20}\cos(\omega_2 t_0)\} - c_d\omega_2\{A_{20}\cos(\omega_2 t_0) - B_{20}\sin(\omega_2 t_0)\} = 0,\end{gathered} \tag{A5}$$

Simplifying and equating the coefficients of $\cos(\omega_2 t_0)$ and $\sin(\omega_2 t_0)$ in Eq. (A5) respectively, the following equations are obtained:

$$\begin{gathered}\frac{dA_{20}}{dt_1} = \frac{4\alpha}{9\omega_2}(\omega_2 - 4\omega_1)A_{10}\sin(\phi t_1) + \frac{4\alpha}{9\omega_2}(\omega_2 - 4\omega_1)B_{10}\cos(\phi t_1) - \frac{\pi^4 P_1^2}{4\omega_2}B_{20}\{2\left(A_{20}^2 + B_{20}^2\right) + \\ \sum_{l=1}^{\infty} l^2\left(A_{l0}^2 + B_{l0}^2\right)\} - \frac{3k_{sn}}{16\omega_2}\left(A_{10}^2 + B_{10}^2\right)B_{20} - \frac{k_{sl}}{2\omega_2}B_{20} - \frac{c_d}{2}A_{20}, \\ \frac{dB_{20}}{dt_1} = -\frac{4\alpha}{9\omega_2}(\omega_2 - 4\omega_1)A_{10}\cos(\phi t_1) + \frac{4\alpha}{9\omega_2}(\omega_2 - 4\omega_1)B_{10}\sin(\phi t_1) + \frac{\pi^4 P_1^2}{4\omega_2}A_{20}\{2\left(A_{20}^2 + B_{20}^2\right) + \\ \sum_{l=1}^{\infty} l^2\left(A_{l0}^2 + B_{l0}^2\right)\} + \frac{3k_{sn}}{16\omega_2}\left(A_{10}^2 + B_{10}^2\right)A_{20} + \frac{k_{sl}}{2\omega_2}A_{20} - \frac{c_d}{2}B_{20}.\end{gathered} \tag{A6}$$

Hence, the coupled system of ordinary differential equations is given by:

$$\begin{aligned}
\frac{dA_{10}}{dt_1} &= -\frac{4\alpha}{9\omega_1}\left(\omega_2-4\omega_1\right)A_{20}\sin\left(\phi t_1\right)+\frac{4\alpha}{9\omega_1}\left(\omega_2-4\omega_1\right)B_{20}\cos\left(\phi t_1\right)-\frac{\pi^4P_1^2}{32\omega_1}B_{10}\{\left(A_{10}^2+B_{10}^2\right)+\\
&\quad 2\sum_{l=1}^{\infty}l^2\left(A_{l0}^2+B_{l0}^2\right)\}-\frac{3k_{sn}}{16\omega_1}\left(A_{20}^2+B_{20}^2\right)B_{10}-\frac{k_{sl}}{2\omega_1}B_{10}-\frac{c_d}{2}A_{10},\\
\frac{dB_{10}}{dt_1} &= -\frac{4\alpha}{9\omega_1}\left(\omega_2-4\omega_1\right)A_{20}\cos\left(\phi t_1\right)-\frac{4\alpha}{9\omega_1}\left(\omega_2-4\omega_1\right)B_{20}\sin\left(\phi t_1\right)+\frac{\pi^4P_1^2}{32\omega_1}A_{10}\{\left(A_{10}^2+B_{10}^2\right)+\\
&\quad 2\sum_{l=1}^{\infty}l^2\left(A_{l0}^2+B_{l0}^2\right)\}+\frac{3k_{sn}}{16\omega_1}\left(A_{20}^2+B_{20}^2\right)A_{10}+\frac{k_{sl}}{2\omega_1}A_{10}-\frac{c_d}{2}B_{10},\\
\frac{dA_{20}}{dt_1} &= \frac{4\alpha}{9\omega_2}\left(\omega_2-4\omega_1\right)A_{10}\sin\left(\phi t_1\right)+\frac{4\alpha}{9\omega_2}\left(\omega_2-4\omega_1\right)B_{10}\cos\left(\phi t_1\right)-\frac{\pi^4P_1^2}{4\omega_2}B_{20}\{2\left(A_{20}^2+B_{20}^2\right)+\\
&\quad \sum_{l=1}^{\infty}l^2\left(A_{l0}^2+B_{l0}^2\right)\}-\frac{3k_{sn}}{16\omega_2}\left(A_{10}^2+B_{10}^2\right)B_{20}-\frac{k_{sl}}{2\omega_2}B_{20}-\frac{c_d}{2}A_{20},\\
\frac{dB_{20}}{dt_1} &= -\frac{4\alpha}{9\omega_2}\left(\omega_2-4\omega_1\right)A_{10}\cos\left(\phi t_1\right)+\frac{4\alpha}{9\omega_2}\left(\omega_2-4\omega_1\right)B_{10}\sin\left(\phi t_1\right)+\frac{\pi^4P_1^2}{4\omega_2}A_{20}\{2\left(A_{20}^2+B_{20}^2\right)+\\
&\quad \sum_{l=1}^{\infty}l^2\left(A_{l0}^2+B_{l0}^2\right)\}+\frac{3k_{sn}}{16\omega_2}\left(A_{10}^2+B_{10}^2\right)A_{20}+\frac{k_s}{2\omega_2}A_{20}-\frac{c_d}{2}B_{20}.
\end{aligned}\tag{A7}$$

Appendix C

In this appendix, the validity of the results is confirmed by comparison with Suweken and Van Horssen [41], which used a similar phase-portrait approach to examine stability. While Suweken and Van Horssen [41] considered only nonlinear vibration without damping, linear and nonlinear elastic foundation effects, setting $c_d=0$, $k_{sl}=0$ and $k_{sn}=0$ in the present model reduces it to the same system given by Suweken and Van Horssen [41]. Under these conditions, the equations and phase portraits match exactly, demonstrating the correctness of the results in this limiting case.

Validation of $\Omega\neq\pm\omega_n\pm\omega_k$(Non-Resonant case)

When damping $c_d=0$, the linear elastic foundation $k_{sl}=0$ and the nonlinear elastic foundation$k_{sn}=0$ in Eq. (28), the solution reduces to the same form as presented by Suweken and Van Horssen [41] and given as:

$$\begin{aligned}
r_k\left(t_1\right) &= C,\\
\phi_k\left(t_1\right) &= -\frac{k^2\pi^4P_1^2}{32\omega_k}C^2\left(k^2+2\sum_{l=1}^{\infty}l^2\right)+\widetilde{C}.
\end{aligned}\tag{A8}$$

Validation of $\Omega=\pm\omega_n\pm\omega_k$(Resonant cases)

For the resonant cases, when damping $c_d=0$, the linear elastic foundation $k_{sl}=0$ and the nonlinear elastic foundation $k_{sn}=0$. The same set of coupled ordinary differential equations are obtained as given by Suweken and Van Horssen [41] and also the corresponding phase portraits agree exactly for the following resonant cases.

Case 1. When $\Omega=\omega_2-\omega_1+\epsilon\phi$

Under these conditions, Eq. (31) reduces to:

$$\begin{aligned}
\frac{dr_1}{dt_1} &= \frac{4\alpha(4\omega_1-\omega_2)}{9\omega_1}\sqrt{\frac{c_1-\omega_1r_1^2}{\omega_2}}\sin(\Phi),\\
\frac{d\Phi}{dt_1} &= \phi+\frac{4\alpha(4\omega_1-\omega_2)}{9}\left(\frac{\sqrt{c_1-\omega_1r_1^2}}{\omega_1\sqrt{\omega_2}r_1}-\frac{r_1}{\sqrt{\omega_2}\sqrt{c_1-\omega_1r_1^2}}\right)\cos(\Phi)+\pi^4P_1^2\{\left(\frac{3}{32\omega_1}-\frac{1}{4\omega_2}\right)r_1^2+\left(\frac{1}{4\omega_1}-\frac{3}{2\omega_2}\right)\frac{c_1-\omega_1r_1^2}{\omega_2}+\\
&\quad \left(\frac{1}{16\omega_1}-\frac{1}{4\omega_2}\right)C^2\sum_{l=3}^{\infty}l^2\},
\end{aligned}\tag{A9}$$

By applying the following rescaling, Eq. (A9) becomes identical in the form, which is given by Suweken and Van Horssen [41]:

$$r_1\left(t_1\right)=\sqrt{\frac{c_2}{\omega_1}}R_1\left(s_2\right),\ s_1=\frac{4\alpha}{9\sqrt{\omega_1\omega_2}}\left(4\omega_1+\omega_2\right)t_1,\ \frac{ds_2}{ds_1}=\frac{1}{R_1\sqrt{R_1^2-1}},\ \Phi\left(t_1\right)=\psi_1(s_2),\tag{A10}$$

which leads to:

$$\begin{aligned} \tfrac{dR_1}{ds_2} &= R_1\left(R_1^2-1\right)\sin\left(\psi_1\right), \\ \tfrac{d\psi_1}{ds_2} &= \left(2R_1^2-1\right)\cos\left(\psi_1\right)-\left(k_1R_1^2+k_2\right)R_1\sqrt{R_1^2-1}, \end{aligned} \tag{A11}$$

with $k_1=\frac{9P_1^2\pi^4\sqrt{\omega_1\omega_2}}{4\alpha(4\omega_1+\omega_2)}\widetilde{k}_j$ for $j=1,2$ where $\widetilde{k_1}=\left(\frac{3}{32\omega_1}+\frac{1}{4\omega_2}\right)\frac{c_2}{\omega_1}+\left(\frac{1}{4\omega_1}+\frac{3}{2\omega_2}\right)\frac{c_2}{\omega_2}$ and $\widetilde{k_2}=-\left(\frac{1}{4\omega_1}+\frac{3}{2\omega_2}\right)\frac{c_2}{\omega_2}-\frac{\phi}{P_1^2\pi^4}+\left(\frac{1}{16\omega_1}+\frac{1}{4\omega_2}\right)C^2\sum_{l=3}^{\infty}l^2$.

The corresponding phase portraits also agree precisely, as illustrated in **Figures A1–A6**.

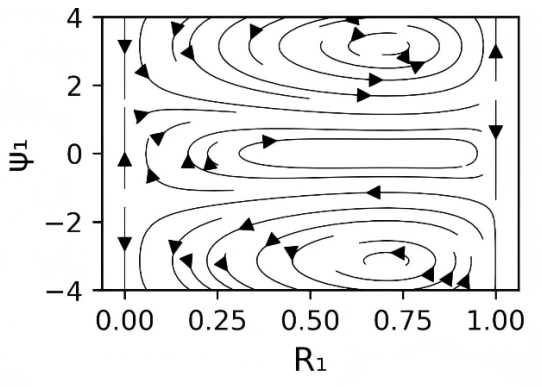

Figure A1. $k_1=4$ and $k_2=-2$.

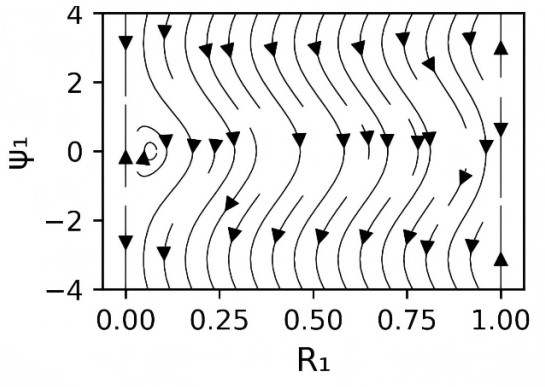

Figure A2. $k_1=9$ and $k_2=-15$.

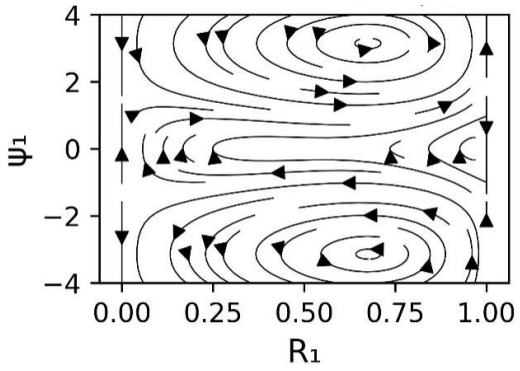

Figure A3. $k_1=6.5$ and $k_2=-2.8$.

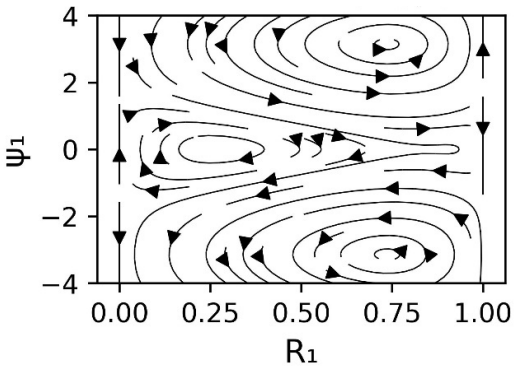

Figure A4. $k_1=6.5$ and $k_2=-3.7$.

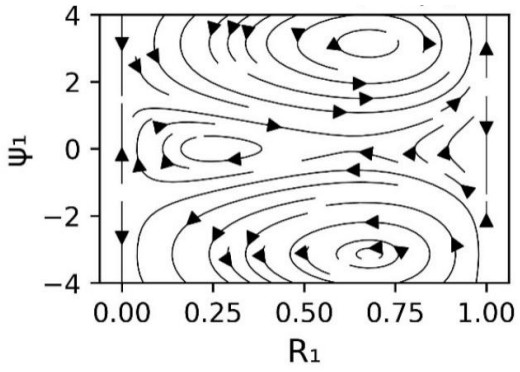

Figure A5. $k_1=9$ and $k_2=-4$.

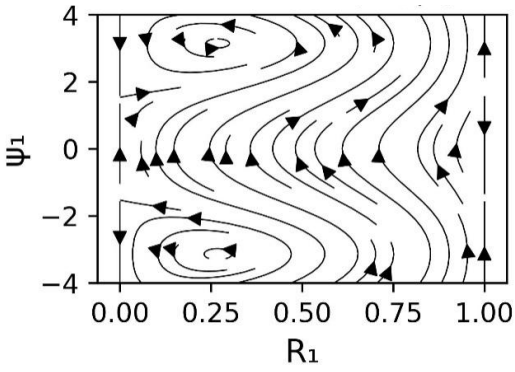

Figure A6. $k_1=4$ and $k_2=3$.

Case 1. When $\Omega = \omega_2 - \omega_1 + \epsilon\phi$

In this case, Eq. (34) reduces to the following form:

$$\begin{gathered}\frac{dr_1}{dt_1} = \frac{4\alpha(4\omega_1+\omega_2)}{9\omega_1}\sqrt{\frac{\omega_1 r_1^2 - c_2}{\omega_2}}\sin(\Phi),\\ \frac{d\Phi}{dt_1} = \phi + \frac{4\alpha(4\omega_1+\omega_2)}{9}\left(\frac{\sqrt{\omega_1 r_1^2-c_2}}{\omega_1\sqrt{\omega_2}r_1} + \frac{r_1}{\sqrt{\omega_2}\sqrt{\omega_1 r_1^2-c_2}}\right)\cos(\Phi) - \pi^4 P_1^2\{\left(\frac{3}{32\omega_1}+\frac{1}{4\omega_2}\right)r_1^2 + \left(\frac{1}{4\omega_1}+\frac{3}{2\omega_2}\right)\frac{\omega_1 r_1^2 - c_2}{\omega_2} + \\ \left(\frac{1}{16\omega_1}+\frac{1}{4\omega_2}\right)C^2\sum_{l=3}^{\infty} l^2\},\end{gathered} \tag{A12}$$

Applying the following rescaling, Eq. (A12) takes the exact same form which is given by Suweken and Van Horssen [41]:

$$r_1(t_1) = \sqrt{\frac{c_1}{\omega_1}}R_1(s_2),\ s_1 = \frac{4\alpha}{9\sqrt{\omega_1\omega_2}}(4\omega_1-\omega_2)t_1,\ \frac{ds_2}{ds_1} = \frac{1}{R_1\sqrt{1-R_1^2}},\Phi(t_1) = \psi_1(s_2), \tag{A13}$$

which yields:

$$\begin{aligned}\frac{dR_1}{ds_2} &= R_1\left(1-R_1^2\right)\sin(\psi_1),\\ \frac{d\psi_1}{ds_2} &= \left(1-2R_1^2\right)\cos(\psi_1) + \left(k_1 R_1^2 + k_2\right)R_1\sqrt{1-R_1^2},\end{aligned} \tag{A14}$$

with $k_1 = \frac{9P_1^2\pi^4\sqrt{\omega_1\omega_2}}{4\alpha(4\omega_1-\omega_2)}\widetilde{k_j}$ for $j = 1, 2$ where $\widetilde{k_1} = \left(\frac{3}{32\omega_1}-\frac{1}{4\omega_2}\right)\frac{c_1}{\omega_1} - \left(\frac{1}{4\omega_1}-\frac{3}{2\omega_2}\right)\frac{c_1}{\omega_2}$ and $\widetilde{k_2} = \left(\frac{1}{4\omega_1}-\frac{3}{2\omega_2}\right)\frac{c_1}{\omega_2} + \frac{\phi}{P_1^2\pi^4} + \left(\frac{1}{16\omega_1}-\frac{1}{4\omega_2}\right)C^2\sum_{l=3}^{\infty} l^2$.

The corresponding phase portraits are also in agreement, as shown in **Figures A7–A12**.

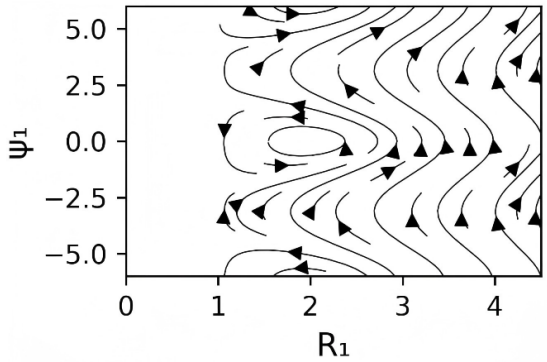

Figure A7. $k_1 = 1$ and $k_2 = -2$.

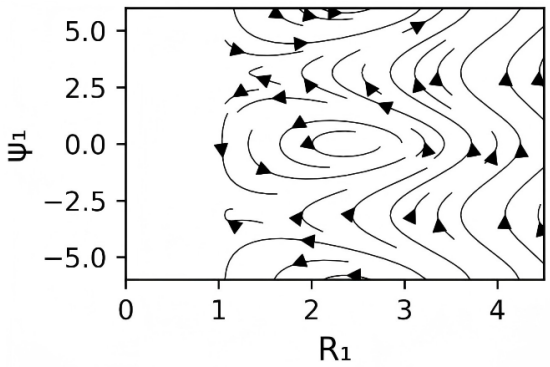

Figure A8. $k_1 = 1$ and $k_2 = -3.802$.

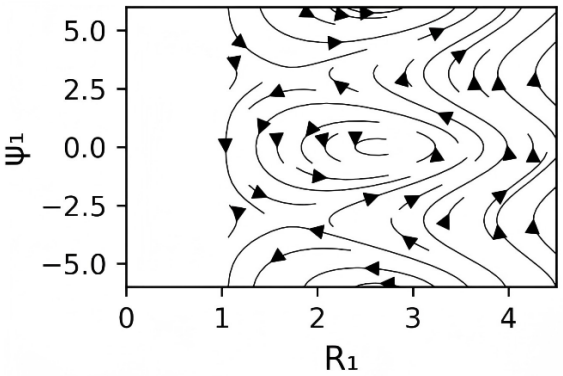

Figure A9. $k_1 = 1$ and $k_2 = -5$.

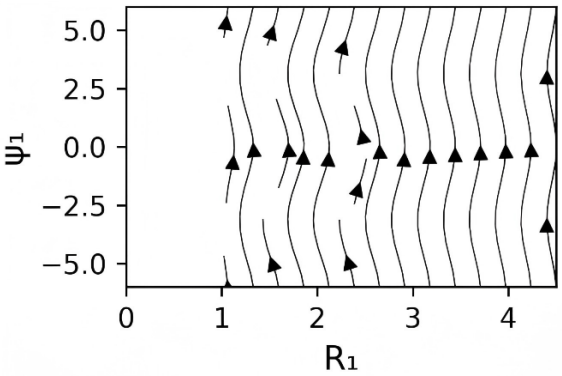

Figure A10. $k_1 = 4$ and $k_2 = 4$.

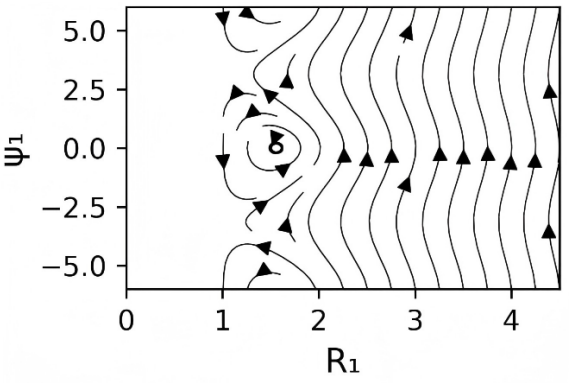

Figure A11. $k_1 = 4$ and $k_2 = -7.657$.

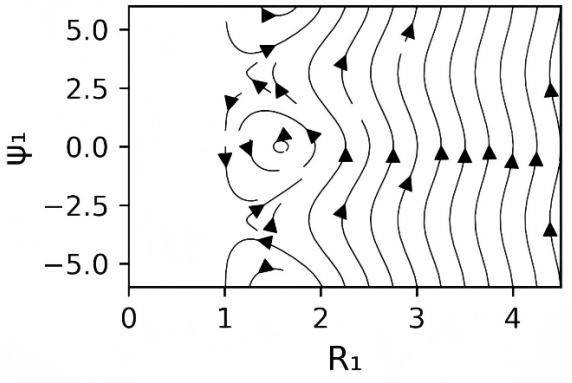

Figure A12. $k_1 = 4$ and $k_2 = -8$.